Chapter One

Introduction

1.1 General view :

Intra fraction motion is an issue that is becoming increasingly important in the era of radiation imaging and guided radiotherapy. Intra fraction motion can be caused by the respiratory, skeletal, muscular, cardiac, and gastrointestinal systems. Of these four systems, much research and development to date has been directed towards accounting for respiratory motion. The management of respiratory motion in radiation oncology is the subject of this work as the respiratory motion affects all tumor sites in the thorax and abdomen (Kitamura et al, 2002; Malone et al, 2000 and Weiss et al, 2003). Figure (1.1) shows the chest movement according to respiration states (Inhalation and Expiration) which cause to chest expands and contracts .

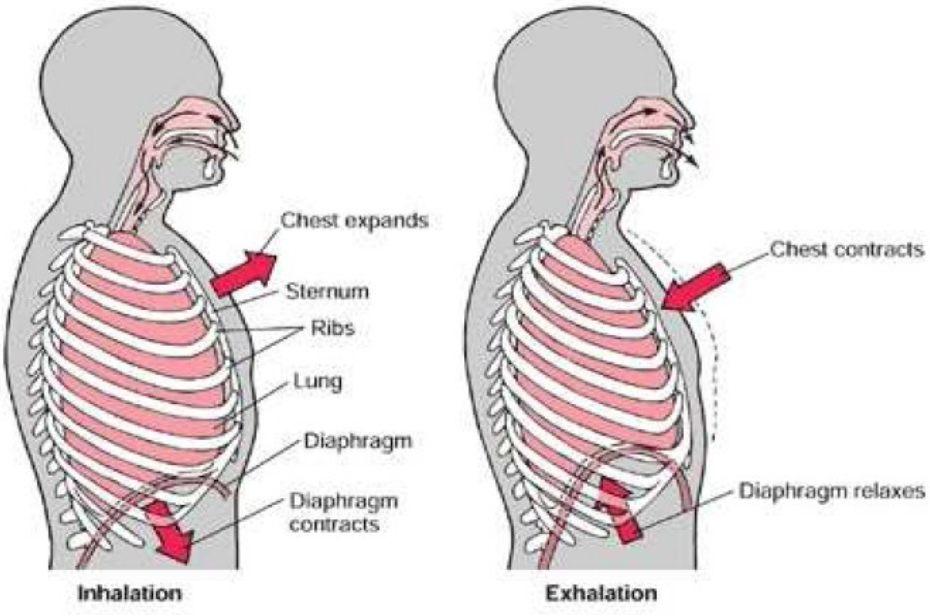

Figure (1.1) Qualitative description of breathing. During the breathing, the bone rotation around the vertebrae makes the thorax volume change, and the diaphragm contraction compresses the viscera, causing the abdominal volume increase.

Such motion has been highlighted and confirmed by some authors as show in Figure (1.1) and (1.2):

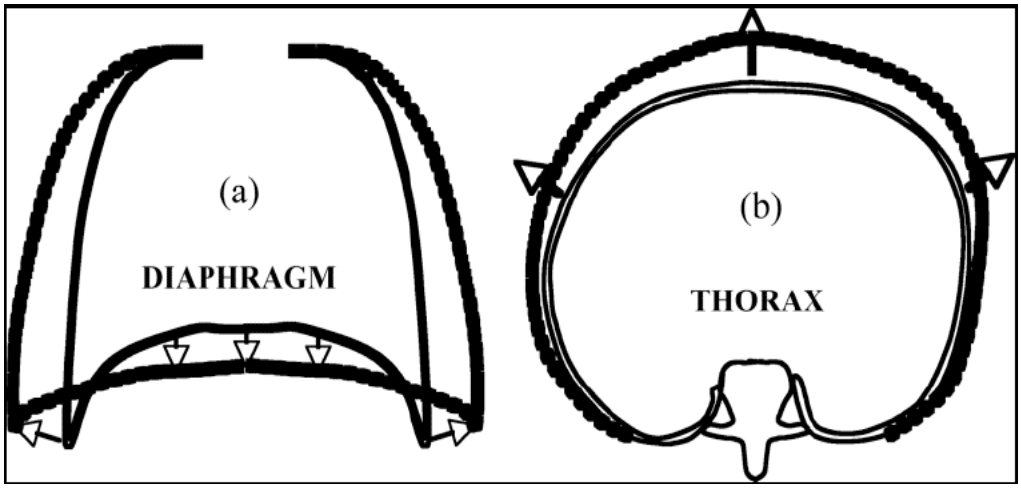

Fig. (1.2) During inhalation, the diaphragm contracts, the abdomen is forced down and forward, and the rib cage is lifted. (b). the intercostals muscles also contract to pull and rotate the ribs, resulting in increasing both the lateral and anterior–posterior (AP) diameters of the thorax (West, 1974).

The motion of human organs due to respiratory effect could influence the administration of radiation dose in Radiotherapy (the treatment of diseases by using radiation such as x-ray, gama-ray or energetic particles).

The radiotherapy is given to cancer patients using Co-60 teletherapy unit or Linear accelerators by collimating suitable field size and directed to site of tumor.

The aim of radiotherapy is to destroy cancer cells with as little damage as possible to normal cells. Radiotherapy can be used to treat many kinds of cancer in most parts of the body. It is particularly effective for head and neck cancers, lung and breast cancers, and cancers in the abdomen and pelvic area. Depending on the type and stage of cancer, radiotherapy has different goals:

- Curative treatment: to cure cancer and reduce the risk of it recurring.
- Palliative treatment: to relieve symptoms such as pain, pressure or bleeding.

In a Co-60 teletherapy machine Figure (3), the radiation source is kept outside the body and the beam is directed on the cancer site. The major components of the machine are Cobalt-60 Source, Source Head, Source Drawer, Collimator, Gantry, Base Housing, Controller and Control Console as shown in table (1). The unit also has a Couch on which the patient is positioned during treatment. Its indexed Patient Positioning System enables quick, accurate and reproducible patient positioning.

However the conventional collimator in Co-60 unit Figure (4) usually designed to offer rectangular field size shape or square, which is fixed according to planned tumor dimension or target volume. While the respiration process would lead to displace the tumor out side the radiation field or could displace the other critical organ in side the radiation field resulting in cancer recurrence due to un-irradiation of the growth target volume (GTV) or critical organ damaging.

The description of target volumes has been mentioned in International Commission on Radiation Units (ICRU) Report 50 (1993), 62 (1999) and 71 (2004). Such reports have been utilized by Radiation therapy centers as shown in Figure (1.3).

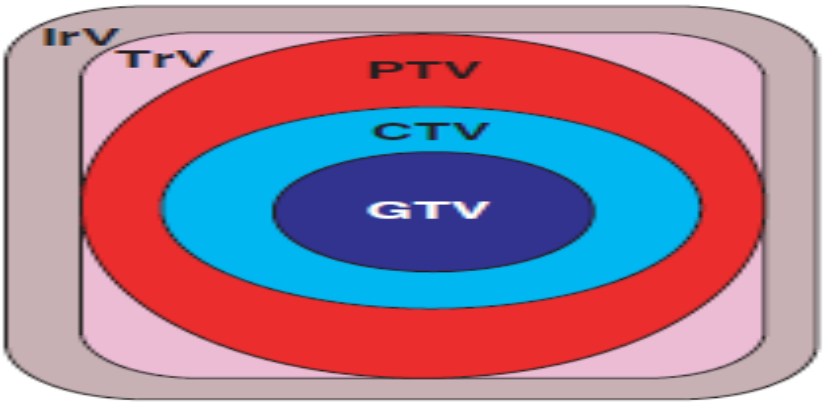

Figure (1.3)ICRU Target volume definitions.

Figure (1.3) ICRU target volume definitions showing GTV, CTV, PTV, treated and irradiated volume. Reproduced with permission from ICRU (1993) Prescribing, Recording and Reporting Photon Beam Therapy. ICRU report 50.

Gross tumor volume (GTV) refers to the primary tumor or other tumor mass shown by clinical examination, at examination under anaesthetic (EUA) or by imaging. GTV is classified by staging systems such as TNM (UICC), AJCC or FIGO. Tumor size, site and shape may appear to vary depending on the imaging technique used and an optimal imaging method for each particular tumor site must therefore also be specified. A GTV may consist of primary tumor (GTV-T) and/or metastatic lymphadenopathy (GTV-N) or distant metastases (GTV-M). GTV always contains the highest tumor cell density and is absent after complete surgical resection.

Clinical target volume (CTV) contains the GTV when present and/or subclinical microscopic disease that has to be eradicated to cure the tumor. CTV definition is based on histological examination of post mortem or surgical specimens assessing extent of tumor cell spread around the gross GTV, as described by Holland et al, (1985) for breast cancer. The GTV-CTV margin is also derived from biological characteristics of the tumor, local recurrence patterns and experience of the radiation oncologist. A CTV containing a primary tumor may lie in continuity with a nodal GTV/CTV to create a CTV-TN (e.g. tonsillar tumor and ipsilateral cervical nodes). When a potentially involved adjacent lymph node which may require elective irradiation lies at a distance from the primary tumor, separate CTV-T and CTV-N are used (Figure 1.4), e.g. an anal tumor and the inguinal nodes.CTV can be denoted by the dose level prescribed, as for example, CTV-T50 for a particular CTV given 50 Gy. For treatment of breast cancer, three CTVs may be used for an individual patient: CTV-T50 (50 Gy is prescribed to the whole

breast); CTV-T66 (66 Gy to the tumor bed); and CTV-N50 (50 Gy to regional lymph nodes). Variation in CTV delineation by the clinician (‘doctor's delineation error’) is the greatest geometrical uncertainty in the whole treatment process.

Studies comparing outlining by radiologists and oncologists have shown a significant inter-observer variability for both the GTV and/or CTV at a variety of tumor sites. This is greater than any intra-observer variation. Published results for nasopharynx, brain, lung, prostate, medulloblastoma and breast all show significant discrepancies in the volumes outlined by different clinicians.

Improvements can be made with training in radiological anatomy which enables clinicians to distinguish blood vessels from lymph nodes and to identify structures accurately on computed tomography (CT) and magnetic resonance imaging (MRI). Joint outlining by radiologists and oncologists can improve consistency and ensure accurate interpretation of imaging of the GTV. Consensus guidelines such as those for defining CTV for head and neck nodes (Gregoire et al, 2000) and pelvic nodes (Taylor et al, 2005) have improved CTV delineation greatly.

When the patient moves or internal organs change in size and shape during a fraction of treatment or between fractions (intra- or inter-fractionally), the position of the CTV may also move. Therefore, to ensure a homogeneous dose to the CTV throughout a fractionated course of irradiation, margins must be added around the CTV. These allow for physiological organ motion (internal margin) and variations in patient positioning and alignment of treatment beams (set-up margin), creating a geometric planning target volume. The planning target volume (PTV) is used in treatment planning to select appropriate beams to ensure that the prescribed dose is actually delivered to the CTV. Variations in organ motion may be small (e.g. brain), larger and predictable (e.g. respiration or cardiac pulsation), or unpredictable (e.g. rectal and bladder filling).

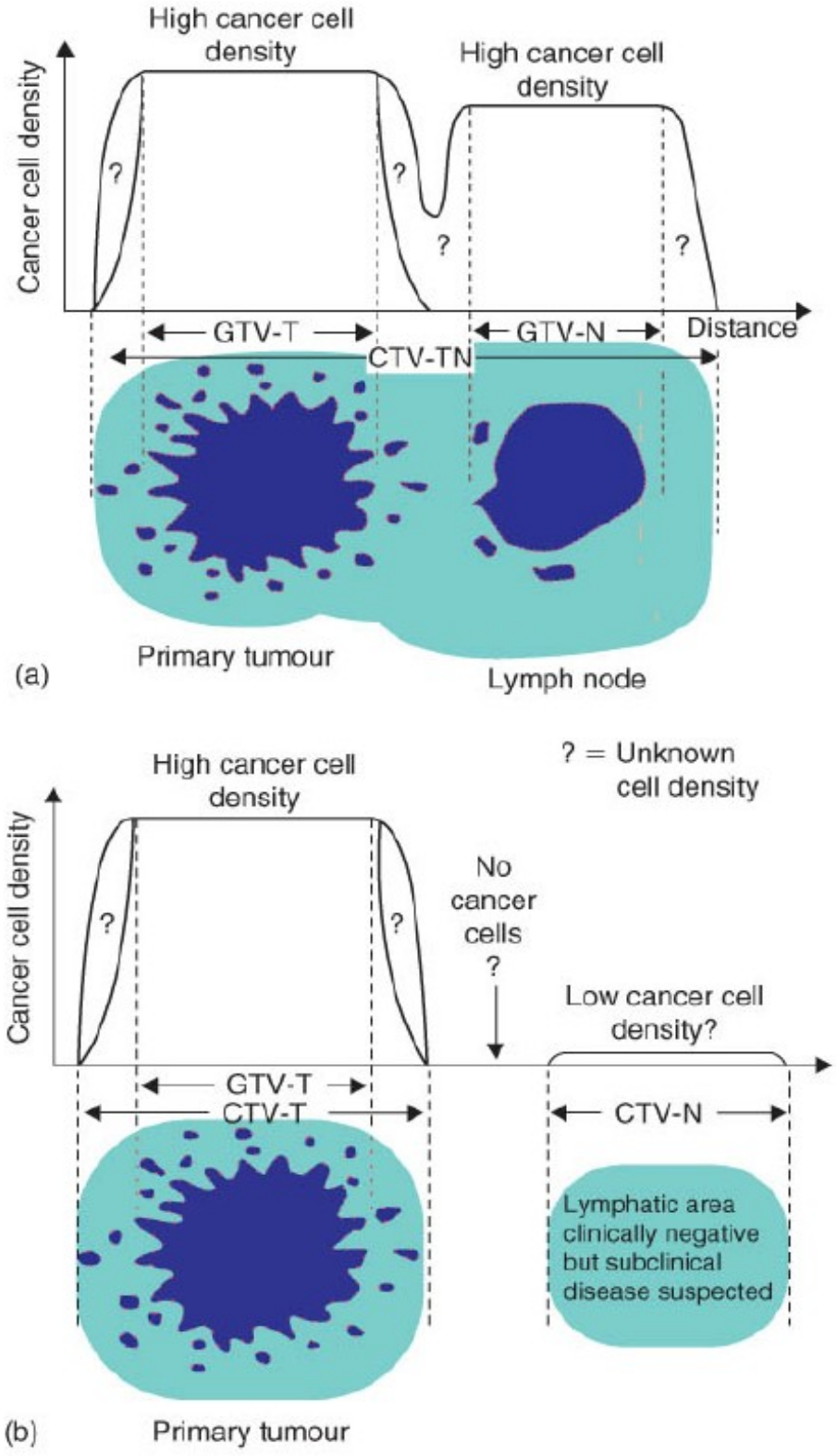

Figure (1.4) ICRU illustrations to show (a) GTV-T plus GTV-N in continuity (CTV-TN) and (b) CTV-T and CTV-N at a distance. Reproduced with permission from ICRU (2004)

Prescribing, Recording and Reporting Electron Beam Therapy. ICRU report 71.

When irradiating lung tumors, the displacement of the CTV caused by respiration can be dealt with in several ways: by increasing the CTV-PTV margin eccentrically to include all CTV positions during a respiratory cycle; by using suspended respiration with a technique such as the active breathing control (ABC) device; or by delivery of radiation using gating or respiratory correlated CT scanning and treatment. Uncertainties from organ motion can also be reduced by using fiducially markers, and published results are available for lung, prostate and breast tumors. Radio-opaque markers are inserted and imaged at localization using CT or MRI, and at treatment verification, using portal films, electronic portal imaging devices (EPIDs) or online cone beam CT image-guided radiotherapy (IGRT). The internal margin therefore allows for inter- and intra-fractional variations in organ position and shape which cannot be eliminated.

The treated volume is the volume of tissue that is planned to receive a specified dose and is enclosed by the isodose surface corresponding to that dose level, e.g. 95 percent. The shape, size and position of the treated volume in relation to the PTV should be recorded to evaluate and interpret local recurrences (in field versus marginal) and complications in normal tissues, which may be outside the PTV but within the treated volume.

The irradiated volume is the volume of tissue that is irradiated to a dose considered significant in terms of normal tissue tolerance,

and is dependent on the treatment technique used. The size of the irradiated volume relative to the treated volume (and integral dose) may increase with increasing numbers of beams, but both volumes can be reduced by beam shaping and conformal therapy. The organs at risk are critical normal tissues whose radiation sensitivity may significantly influence treatment planning and/or prescribed dose. Any movements of the organs at risk (OAR) or uncertainties of set-up may be accounted for with a margin similar to the principles for PTV, to create a planning organ at risk

volume (PRV). The size of the margin may vary in different directions. Where a

PTV and PRV are close or overlap a clinical decision about relative risks of tumor relapse or normal tissue damage must be made. Shielding of parts of normal organs is possible with the use of multi-leaf collimation (MLC). Dose–volume histograms (DVHs) are used to calculate normal tissue dose distributions.

Figure (1.5) Photograph of the Theratron 780C Co-60 Radiotherapy unit, adapted from Joshi et al. (2008).

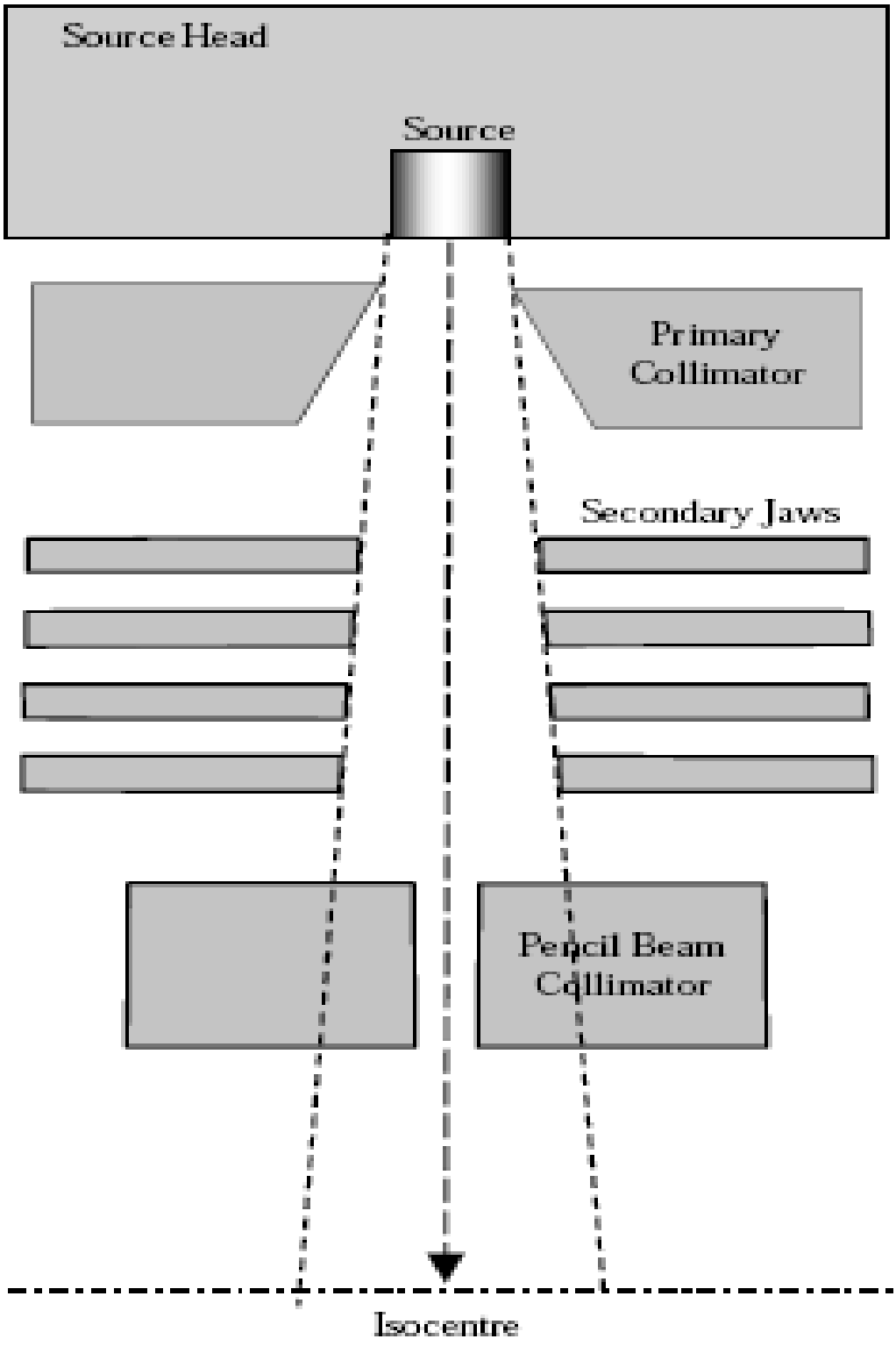

Figure (1.6) the schematic diagram of the geometry inside its treatment head. The geometry of the treatment head is adapted from Joshi et al. (2008).

Table (1.1) Specifications of Co-60 teletherapy machine :

Source head	Up to 200 RMM
Source to isocentre distance	80 cm
Floor to isocentre distance	115 cm
Collimator	Field size min: 0 x 0 cm at 80 cm Field size max: 35 x 35 cm at 80 cm Rotation: 360 degrees a round its central axis Field size indicator: digital display Field size adjustment: motorized
Source to Skin Distance Indicator	Optically projected over the field under treatment (60-100 cm)
Patient Support Assembly Motions	Vertical: 70 cm to 170 cm from floor Longitudinal: 70 cm Lateral: 620 cm Couch rotation: +/- 95 degrees
Control console	Machine health status of AC power, Battery, Door, Wedge, Key and Air Displays exposed time and set time Source position indicator Emergency stop switch

	Patient and treatment database Treatment data interlock Gantry, Collimator and Couch motions
Hand control	Gantry ,Collimatorand Couch positions Room lights, Laser Lights Emergency Stop switch
Automatic collimator closure	Will close the Collimator jaws to Zero Field size in case of source movement irregularities

1.2 Problem statement:

The movement of the GTV due to breathing (inspiration\expiration) will cause two problems as shown below which represent the problem of the research :-

1-The GTV moves partially side away from the radiation field i.e. receiving insufficient radiation dose.
2-The critical organ will be displaced into the radiation field (damage will be occurred to healthy tosses).

1.3 Objectives of the study:

The objectives of this research are to :-

1. Learn and study about electronic components behavior (properties) to be selected to design an adaptive real time intelligent control system for Co-60 diaphragm.
2. Use (select) a pressure sensor device for physiological motion.
3. Feed in the diaphragm with pulsating signal that generated from abdomin physiological motion.

4. Using code vision program for simulating the adaptive system operation results.
5. Obtain real time field irradiation for organs affected by respiration e.g. Bronchus carcinoma or esophageal carcinoma or prostatic carcinoma.

1.4 Methodolgy:

Designing an adaptive electronic control system based on pressure sensor to sense the mechanical movement of the chest or abdomen ,during breathing (inspiration and expiration) and then translate this mechanical movement into electrical signal (using sensor).

This a small analoge signal should be amplified (using amplifier) and then converted to digital signal (using analoge to digital converter circuit) see figure(1.7).

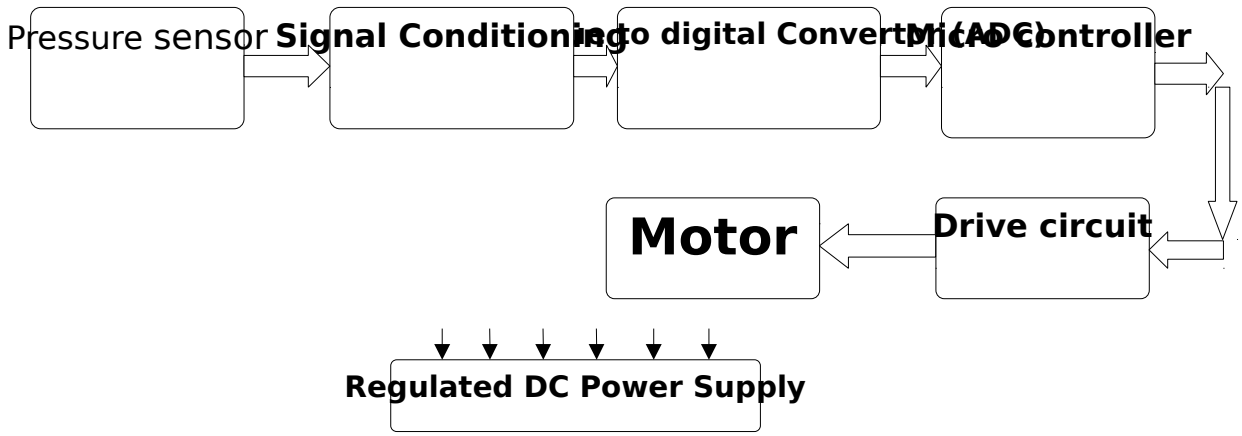

Figure(1.7) shows the system block diagram

This signal should be feeded back to the motor collimator (diaphragm) of the cobalt-60 inform of pulsating signal , in order to cause the diaphragm moves according to the movement of the vital organ motion that been irradiated at the same moment ,

i.e. to make the diaphragm movement mimic (simulate) the movement of the organ motion (displacement) at really time.

So, to fulfill real time accurately, intelligent micro-controller circuit should be used and simulation program should be run before constructing the circuit.

1.5 Thesis layout:

This research consist of Seven chapters. Chapter one is an introduction..Chapter two is highlight the literature review . Chapter three is the cobalt-60 and collimator construction features. Chapter four deals with the proposed system selected devices behaviours. Chapter Five deals with Methodology. Chapter Sex shows the circuit design results and discussion. Chapter Seven will include the conclusion and recommendation.

Chapter Two

Literature Review

Such shortening in Co-60 unit (fixed conventional diaphragm in X-Y direction) and respiration process that affecting passively in radiotherapy process has been overcome by some attempts enumerated in previous studies highlighted as shown below :

1-Some attempts introduced by some authors to overcome problem attributed to organs motion in radiotherapy (Co-60) are so limited. And in this realm ICRU Report 50 (approved in ICRU 62), suggested that to overcome the motion of organs, the irradiated area could include the Gross Tumor Volume (GTV), Clinical Tumor Volume (CTV), Internal Planning Target Volume (IPTV) with Internal Margin (IM), Planning Target Volume (PTV) with Setup Margin (SM), and Organs at Risk (OAR), these volumes are shown in Figure (2.1) :

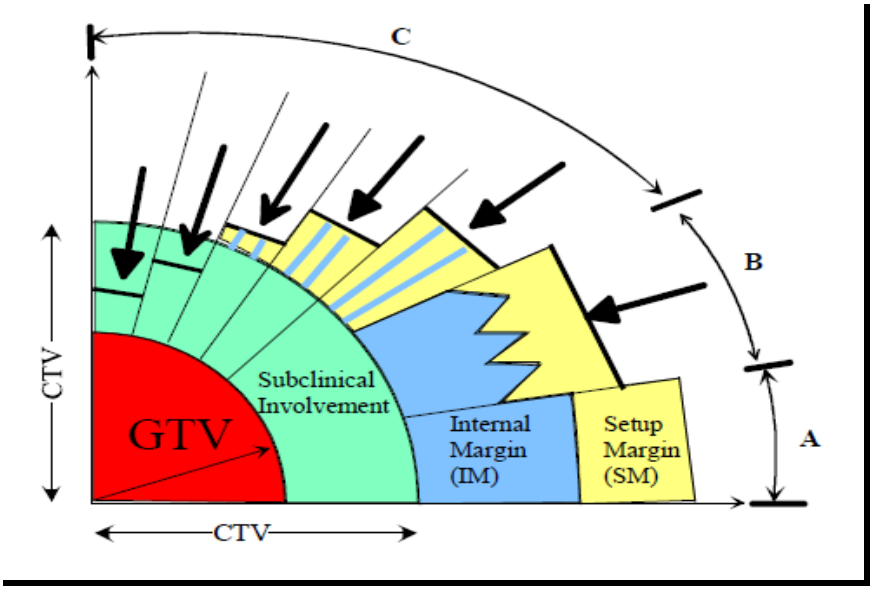

Figure (2.1) Definitions of treatment volumes as defined by ICRU-62 showing their relation by scenarios A, B and C.

2-Other attempt has been introduced by Valicenti et al (1999), Yamamoto et al (1999) which was depending on the imaging modality that visualize the tumor margin then the field size would be open relatively and concisely.

3- Also in most recent machines there is a multi leave collimator MLC system which is adjusted to mimic the shape of the tumor outline, but still the organ motion is persisting. The design of MLC has been shown in Figure (2.2) .

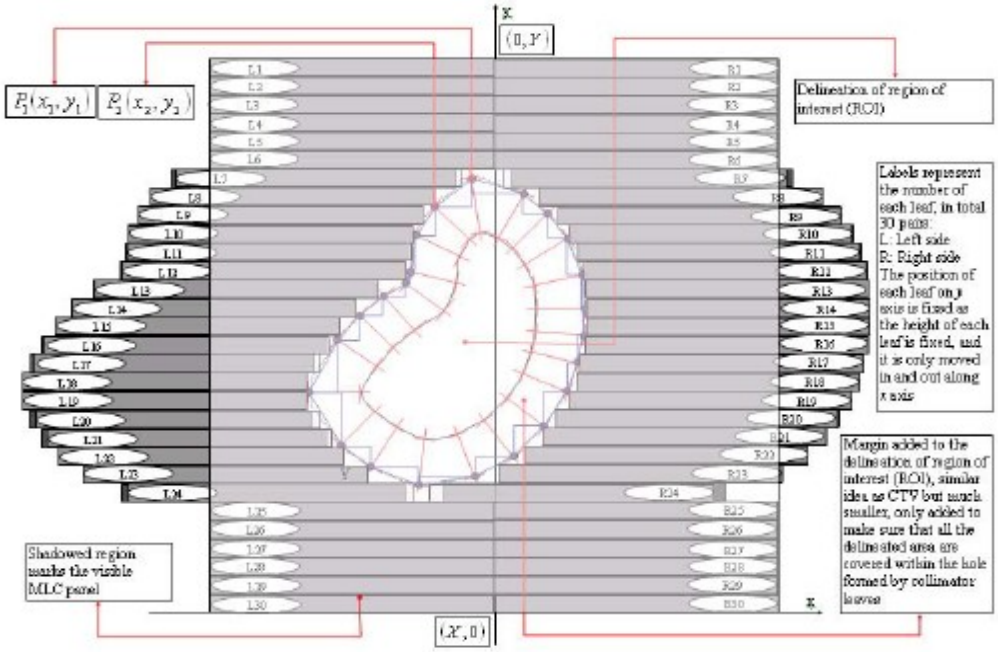

Figure (2.2) shows the design of MLC trigonometry (Su et al,2007).

4-The organ motion problem in radiotherapy could be managed by introducing an innovated real time diaphragm sensor excerpted from the fundamental of net work sensor (Sitharama et al, 2010).

5-In the same realm of trying to manage the problem of respiration motion inradiation therapy, Jun et al, (2009) introduce a concept of Synchronized Moving Aperture Radiation Therapy (SMART), that uperimposinthetumor motion.The basic idea of SMART is to synchronize the moving radiation beam apertureformed by a dynamic multileaf collimator (DMLC) with the tumor motion induced by respiration; however with this concept there were a shower of electron being ejected and leading to skin burn.

6-On the other hand Seungwoo et al, (2009) used a target-tracking radiation-therapy (RT) system that tracks the movement of a treatment target resulting from internal organ movement. The developed radiation-therapy system determines the limit of the MLC (multileaf collimator) movement range with an acquired maximum displacement value of target movement during the radiotherapy planning stage and moves the MLC to continuously detect and synchronize the displacement of the abdominal by using a Charged Coupled Device (CCD) camera monitoring system during real-time RT treatment.

The system consists of a Co-60 teletherapy unit , an abdominal displacement detection system to correlate the movement of internal organs, and a MLC moving stage synchronized with the abdominal displacement.

7-Following the ICRU recommendations (ICRU Report 50, 1993; ICRU Report 62, 1999), radiotherapists have to decide the margins around the clinical target volume (CTV) to accommodate uncertainties in the treatment planning and delivery process, which also include uncertainties due to organ motion. At present, the precise delineation of the target volume that requires the 3D treatment calculation technology is limited by the physiological organ motion and by the daily patient set-up inaccuracies (McCarter and Beckhan, 2000).

Both sources of uncertainty in the target position and size have great influence in the dose delivered to the tumor and surrounding critical organs, and can cause important

modifications of tumor control probability and complications to healthy tissue (Urie et al, 1991).

8-some considerable studies for instance: Sergio et al, (2004) introduce study aboutan Analysis and evaluation of periodic physiological organ motion in radiotherapy treatments, in which a system for the detection and quantification of periodic physiologic movements (breathing and cardiac movement) for each individual patient in a way that can be incorporated to the calculation prior to the treatment is developed. The system is based on real-time acquisition of digital fluoroscopic image sequences of 1 min duration while the patient is freely breathing. An automatic analysis of such sequences allows the accurate computing of the frequency and amplitude of the periodic movement under investigation.

The physiologic organ motion can be classified, according to their temporal
behavior, in: (i) non-periodic motion, produced by the filling status of structures
such as the bladder or the rectum, (ii) periodic motion, due to breathing and cardiac motion (these movements are repeated many times during a single treatment session), and (iii) quasi-periodic motion, like the peristaltic movement of the stomach (Sergio et al, 2004). The largest variation in organ position and shape during radiotherapy is due to breathing. Moreover, its high frequency in comparison with other movements makes essential to take it into account, since any irradiation volume wrongly estimated will be kept during the whole treatment.

The source for target motion is the bio-mechanical activities of the human body. The bio-mechanical action of any skeletal muscle is essentially determined by the anatomy of the muscle and by the structures it displaces when it contracts. The intercostals muscles are morphologically and functionally skeletal muscles, and the primary effect of their contraction is to displace the ribs and thereby to alter the configuration of the rib cage (Andre et al, 2005) and further more displacing the internal organs in the chest (Heart, Lungs, Esophagus).

Set-up uncertainties can be reduced via immobilization techniques and careful daily repositioning of the patient using portal imaging and alignment tools. But tools to include the effect of organ motion in the treatment planning are still needed.

Expansion of the rib cage and abdominal wall are prominent features of the inspiratory phase of the breathing cycle. The expansion of the abdominal wall is produced by the action of the diaphragm. Thus, as the diaphragm is activated, its muscle fibers shorten and its dome (which corresponds essentially to the central tendon) moves in the caudal direction, pushing the abdominal viscera (Stomach, small/large bowel, liver, spleen … etc) caudally and displacing the abdominal wall outward. Such bio-mechanical actions have been reported by some authors (Strohl et al, 1984; Gandevia et al, 1996; Estenne and Troyer, 1985; Sergio et al, 2004). However in view of studying such bio-mechanical activities, also there are

If respiratory motion is not accounted for, as is the case when conventional radiotherapy techniques are applied in thoracic and abdominal sites, it causes artifacts during image acquisition. These artifacts cause distortion of the target volume and

incorrect positional and volumetric information. These motion artifacts occur because different parts of the object move in and out of the computed tomography (CT) slice window during image acquisition. Artifacts can be generated within a slice, since CT reconstruction algorithms assume that the imaged anatomy is invariant during data acquisition (Chen et al, 2004).

There are significant differences in organ motion during quiet (shallow) and deep breathing. Therefore, some of the observers have distinguished their measurements by breathing mode. Generally, abdominal organ motion is in the SI direction, with no more than a 2-mm displacement in the AP and lateral directions. However, in some individuals, the kidneys show more complex patterns. Lung tumor motions generally show a much greater variation in the trajectory of motion (Harauz and Bronskill, 1999). Stevens et al, (2001) found that out of 22 lung tumor patients, 10 subjects showed

no tumor motion in the SI direction. Of the remaining 12 subjects, the average SI

displacement was anywhere from 3 to 22 mm (mean 8 +/– 4 mm). They found no correlation between the occurrences or magnitude of tumor motion and tumor size, location, or pulmonary function, suggesting that tumor motion should be assessed individually.

Barnes et al, (2001) found the average motion of tumors in the lower lung lobe to be significantly greater than that in the middle lobe, upper lobe, or mediastinal tumors (18.5-mm vs. 7.5-mm average SI displacement). This observation has generally been

corroborated by other observations, although the individual ranges of motion are such that some individuals will show less motion in the SI direction than others will show in the AP and left–right directions.

At the time of writing, the most detailed lung tumor-motion data reported in the literature comes from the measurements of Seppenwoolde et al, (2002) who measured 3-D trajectories for 20 patients via dual real-time fluoroscopic imaging of a fiducially marker implanted in or near the tumor. They observed hysteresis in the trajectories of half the patients, amounting to a 1- to 5-mm separation of the trajectories during inhalation and exhalation, with 4 out of 20 patients exceeding a 2-mm separation. This indicates that in cases where high accuracy is required in dose alignment, a real-time tracking or gating process based on surrogate breathing signals should not only correlate with the tumor's motion along each axis with the breathing signal, but should have knowledge of the respiratory phase, because the phase difference is what leads to the hysteresis effect. Motion trajectories during radiotherapy of lung tumors, measured using implanted gold markers, are depicted. The amount of motion ranges from a 1-mm displacement to more than a 2-cm displacement. Furthermore, it can be seen that the motion is nonlinear for about half of the fiducially markers. The majority of the fiducially markers (78% in this study) move with less than a 1cm range of motion. Similar results, based on portal imaging studies, have been reported. (E implemented in most clinics is to acquire both inhale and exhale gated or breath-hold CT scans of the patient during the CT simulation session (Balter et al, 1998).

Taking both inhale and exhale CT scans will more than double the CT A solution to obtaining a tumor-encompassing volume that can be scanning time and relies on the patient's ability to hold his or her breath reproducibly. Two scans will be obtained; thus, image fusion and extra contouring are required. For lung tumors, the maximum intensity projection (MIP) too available in most visualization systems can be used to obtain the tumor-motion–encompassing volume provided there is no mediastinal tumor involvement (Underberg et al, 2005).

The advantage of this approach over the slow scanning method mentioned above is that the blurring caused by the motion present during FB is significantly reduced during breath-hold. Dose calculation should be performed on the CT data set that is most appropriate for the particular patient, e.g., exhale CT for patients generally spending more time at exhale than inhale. The exhale scan will tend to underestimate the lung volumes and, hence, overestimate the percentage of lung volume receiving a specific dose. To save time, a free-breathing CT could be used for the entire scan region (typically including the entire thoracic cavity), with either breath-hold or gated CT scans at inhale and exhale of a scan length sufficient to cover the tumor volume to determine range of motion of the GTV. Some form of respiratory monitoring is necessary to verify gated or breath-hold constancy and to ensure that the scans are representative of the patient's normal breathing range (Sonke et al, 2005).

Breath-hold scans can also potentially be used for respiratory-gated delivery, however, it should be noted that a respiratory-gated CT scan is preferred over a breath-hold scan at the same respiratory position, because the predominant

respiratory muscles can be different for breath-hold and FB (e.g., intercostal vs. diaphragm), and any tumor lag (relative to the external monitor) occurring during FB will be absent during breath-hold (Lu et al, 2005).

Cone-beam kVCT has recently been established as an available tool on a radiotherapy linac, the concept being that a kVCT scan recorded just before treatment can be compared with the planning CT scan and adjustments made to compensate for mispositioning. Generally, however, a kVCT scan takes typically tens of seconds to record and again tens of seconds to reconstruct (although reconstruction can take place during the scanning period). Since this scanning time is considerably longer than the breathing period the resulting kVCT scans would be blurred if no further action were taken. Sonke et al, (2005) have developed a method to extract the breathing signal from each projection based on a measurement of the projected position of the diaphragm. Then the projection data were re-sorted a-posteriori into just eight phases of the breathing cycle and these subsets of data were used to make eight kVCT scans which, viewed as a set, constitute a 4D kVCT reconstruction. Of course the signal-to noise ratio will deteriorate as a result of the fact that fewer projections now comprise each reconstruction. However, it was found that signal-to-noise ratio did not deteriorate to the point that the organs were unable to be identified. Careful experiments were made with a phantom to show that the phase-re-sorted kVCT reconstructions did correspond well with the equivalent kVCT reconstructions of static phantoms at the same breathing phase. A promising

solution for obtaining high-quality CT data in the presence of respiratory motion is 4-D CT or respiration-correlated CT (conventional and cone-beam approaches) (Rietzel et al, 2005).

Four-dimensional data can be analyzed to determine the mean tumor position, tumor range of motion for treatment planning and the relation of tumor trajectory

to other organs and to a respiration monitor (Mageras et al, 2004).

A limitation of 4-D CT is that it is affected by variations in respiratory patterns during acquisition. Breathing-training techniques have been developed however even with these techniques artifacts can be observed. A schematic of 4D CT using a ciné acquisition process is shown in Figure (2.3) (Keall et al, 2004).

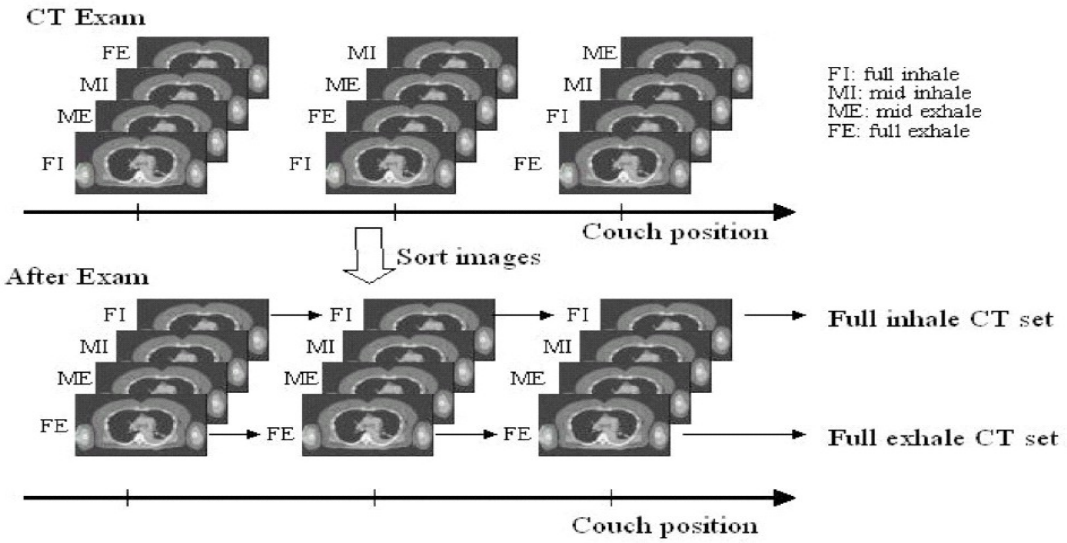

Figure (2.3) A schematic of the 4-D CT process using a ciné acquisition. Images are acquired at each couch position for many respiratory phases.

A 4-D CT scan can be obtained in approximately 1 minute of scanning time with a 16-slice CT scanner. Generally 8 to 25

complete CT datasets are reconstructed, the optimal use of which has yet to be determined. Four-dimensional CT can be used to reconstruct inhale, exhale, and slow CT scans. If 4-D CT is used for these purposes, the procedures described above can be followed. The MIP tool, as mentioned above, may be useful in obtaining the tumor-motion–encompassing target volume (Underberg et al, 2004).

Four-dimensional respiratory-correlated computed tomography (4D RCCT) has been widely used for studying organ motion. The current standard practice is to use phase binned images. However, the phase binning algorithm assumes that the patient has a periodic breathing pattern. When the patient's breathing is irregular, this assumption breaks down and significant image artifacts like those

shown in Figure (2.4) are introduced. In a recent extensive study, Yamamoto et al,

(2001) found that 90% of 4D RCCT patients had at least one artifact. Amplitude binning algorithms have been developed as a way to alleviate these artifacts by assuming that the underlying anatomical configuration is correlated to the amplitude of the breathing signal. This method reduces binning artifacts but since data is not acquired at all breathing amplitudes the images often have some

missing slices. Deformable image registration has been shown to be useful in tracking organ motion in artifact-free 4D RCCT images. Such methods may be used with either phase or amplitude binned images, but is challenged in the presence of binning artifacts.

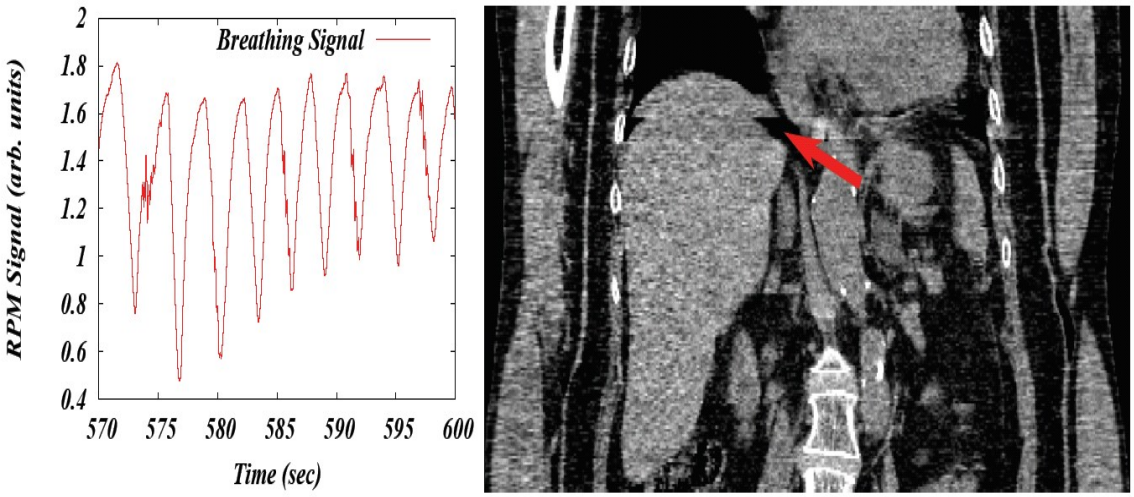

Figure (2.4) Non-periodic patient breathing pattern (left) and image artifacts introduced by phase binning (right).

So, althow some attempts by recearchers were done , still the problem of mechanical organ motion in radiotherapy is not overcome totally, so in this thesis we hope to share solving of this problem by designing an intelligent electronic control circuit for Real-time Collimator in Co-60 Teletherapy Machine is considered as a circuit for feeding up the conventional collimator of Co-60

teletherapy machine collimator with electrical pulses to enable the collimator motors motion (x, y) varying according to variation of the vital organ motion on the spot.

Chapter Three

Cobalt-60 And Collimator Construction features

3-1 Cobalt-60:

Cobalt 60 is produced in a nuclear reactor by bombarding ^{59}Co with neutrons. It has a half life of 5.3 years and decays by negative beta emission to metastable ^{60}Ni. This rapidly releases a gamma ray of either 1.17 or 1.33 MeV to reach a stable state. So the radiotherapy machine is named after cobalt-60(Co-60) .
The source typically has an activity of 185 – 370 MBq, giving a dose rate at 80 cm of 1 – 2 Gy/minute. The Cobalt 60 source is usually replaced before a single half life has elapsed.

Cobalt machines use high energy rays produced by a small (usually 2 cm) radioactive cobalt60-cube placed inside the head of the machine. In “off”-position the cube is deep inside the head. When the machine is turned “on”, the cobalt is moved over an exit port and the beams are directed on the patient.

3.1.1 Construction of a Co-60 Teletherapy Unit:

Gamma ray treatment machines are known as teletherapy units. The patient is placed on the table, with the part intended to be irradiated lying under the head. The head can be moved by means of the gantry to deliver the beam from different positions as seen in figure (3-1).

Figure (3-1) Shows the patient under treatment.

The components of a cobalt-60 machine are as shown in figure (3-2):

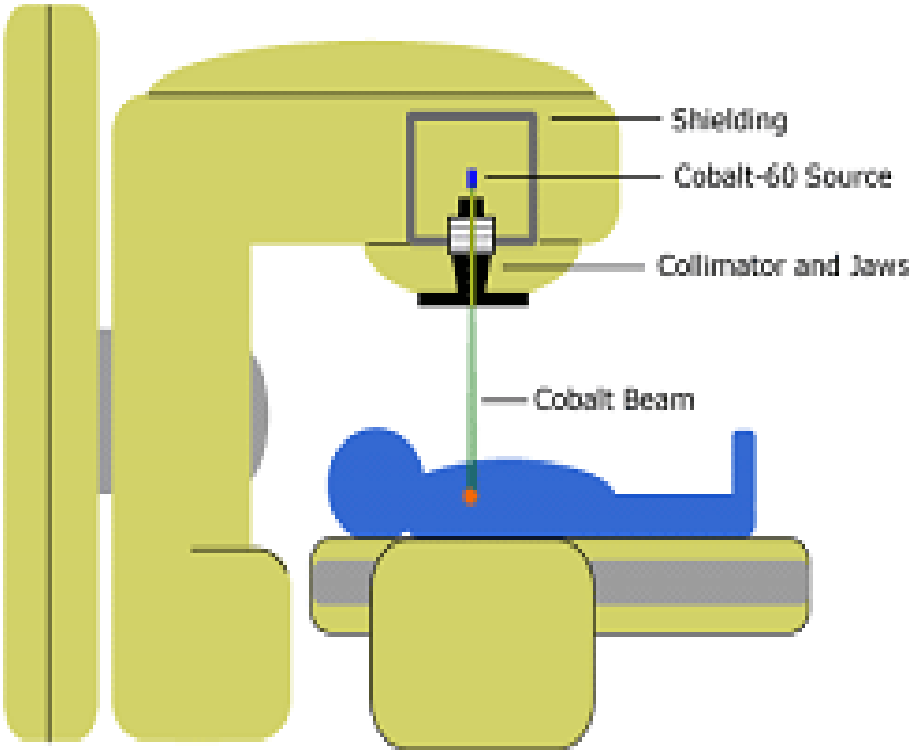

Figure (3-2) shows the main components of Co-60 machine.

- A radioactive source, in this case Co-60, which is housed in a steel capsule.

- Source housing, which includes the primary beam collimator to prevent unwanted radiation emission. The source housing can also shift the source to allow gamma rays to exit the unit through the collimator aperture.
- A gantry (in isocentric machines) to allow the source to rotate around a fixed position. The SAD is usually 80 or 100 cm. The gantry is typically attached to a stand which houses motors and monitoring equipment.
- A patient support assembly or patient couch which allows the patient to be positioned in the desired position.
- A bunker to protect staff, patients and the general public from unnecessary radiation exposure
- A machine console outside the bunker which allows therapists to operate the machine remotely.

3-2 A collimator :

Is a device that narrows a beam of particles or waves. To "narrow" can mean either to cause the directions of motion to become more aligned in a specific direction (i.e., make **collimated** light or parallel rays), or to cause the spatial cross section of the beam to become smaller (beam limiting device) see figure(3.3).

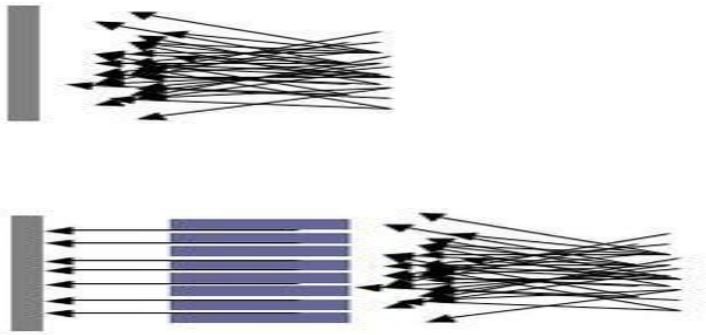

Figure (3.3) shows the general collimting idea.

3.2.1 Collimator main parts in Co-60:

In radiation therapy machine the size and orientation of the radiation beam is controlled by the collimator assembly. Two pairs of motorized jaws generate rectangular field of desired size. The collimator at the exit port allows the use of different square and rectangular field sizes between 3,5 x 3,5 cm and 32 x 32 cm. See figure (3.4) that show the collimator X ,Y jaws and other accessories.

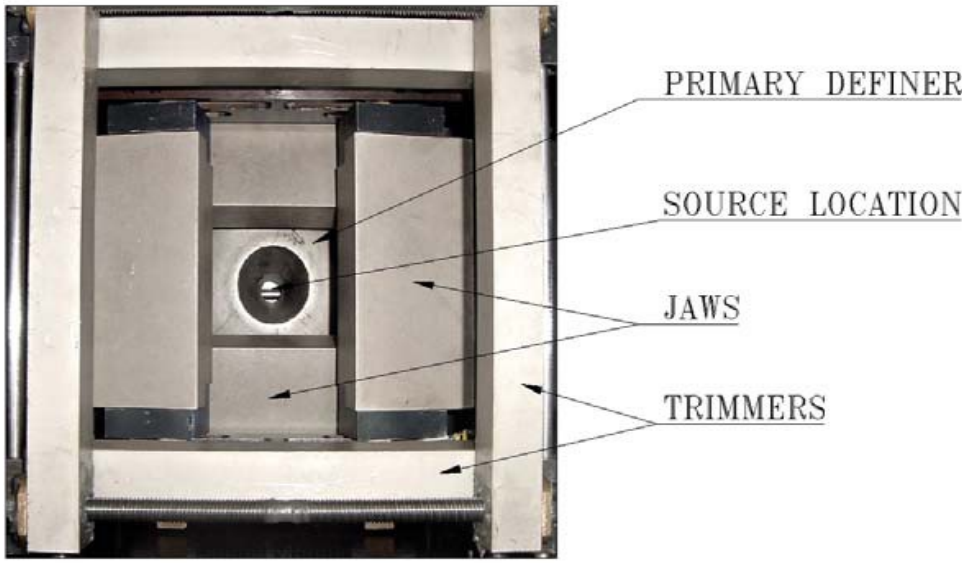

Figure (3.4) Shows X-jaws and Y-jaws collimator .

Fully closable collimator is a unique feature of the machine. It is an improvement over the traditional designs using intermeshing

leaves. In case of any emergency, the collimator gets closed automatically. This ensures improved safety against leakage radiation during accidental situations. Using this machine, it is possible to
deliver radiation beam on a field smaller than the typical 5cmx5cm field size.

The radiation field can be visualized by a high intensity light during patient positioning. The centre of the radiation field is indicated by the collimator cross hairs . The source to skin distance is shown by an optical distance indicator. Two sets of trimmers are provided to decrease the penumbra of the beam.
The lower pad of the collimator is prepared to receive wedge filters and shadow tray for the beam shaping lead blocks. Collimator and trimmers are made of uranium to reduce size. See figure (3.5).

Figure (3.5) shows the patient positioning .

The size of the radiation beam is controlled by the collimator assembly. Two pairs of motorized uranium jaws generate rectangular field of required size. See figure(3.6)

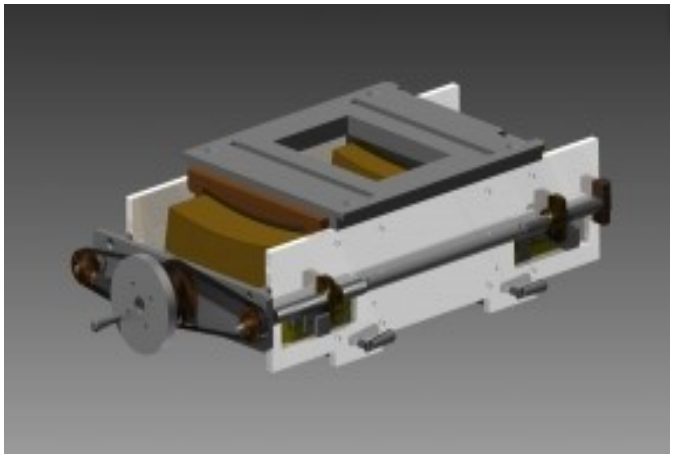

Figure (3.6) Shows the adjustable collimator.

The patient is placed on the table, with the part intended to be irradiated lying under the head. The head can be moved by means of the gantry to deliver the beam from different positions. That is to say the collimator can be rotated around the radiation beam axis. Figure (3.7) shows the collimator that can be adjusted to square or rectangular form at deferent positions.

Figure (3.7) Shows rectangular collimator beside image monitor.

The collimator precisely adjusts the radiation beam to the shape of the tumor to make sure that the surrounding normal tissue is spared. So, the goal of any precision radiotherapy of cancer is to deliver the highest possible radiation dose to the tumor while sparing the surrounding normal tissue .This makes the collimator is a big issue in this research.

Chapter Four

Materials (System Selected Devices)

4.1 General View For Components Used:

The adaptive control system for the proposed design includes the following components after been studied their characteristics and behaviors then selected carefully to construct the system (ttp://www.engineersgarage.com/electronic-components/ 2012 EngineersGarage) as follows:

4.2 Sensors:

A dictionary definition of 'sensor' is `a device that detects a change in a physical stimulus and turns it into a signal which can be measured or recorded.

A corresponding definition of 'transducer' is 'a device that transfers power from one system to another in the same or in the different form.

Transducer = Sensor + Signal conditioning circuit.

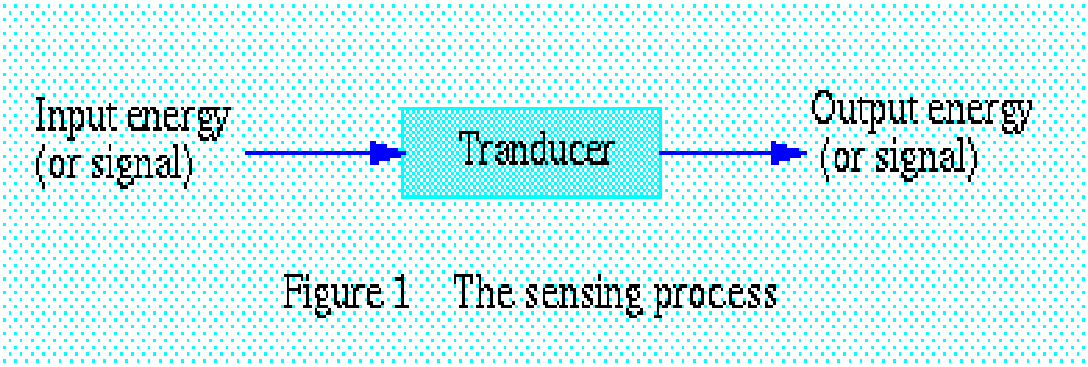

Figure (4.1) Shows the sensing process in terms of energy conversion

The form of the output signal will often be a voltage analogous to the input signal, though sometimes it may be a wave form whose frequency is proportional to the input or a pulse train containing the information in some other form.To look at a sensor , consider all of its properties, such as stimulus, specifications, physical phenomenon, and conversion mechanism, material and application field.

Selection criteria depend on many factors, such as availability, cost, and power be done only after all variables are considered.

4.2.1 Performance Criteria pressure sensor :

1- Accuracy: - The difference between a measurement reading and the true value of that measurement.

2- Error: - The amount of deviation from a standard or specification. Errors should be eliminated in the measuring process.

3- Hysteresis:- The delay between the action and reaction of a measuring instrument. Hysteresis is the amount of error that results when this action occurs.

4- Repeatability: - The ability to obtain consistent results when measuring the same part with the same measuring instrument.

5- Resolution: - The smallest change in a measured value that the instrument can detect. Resolution is also known as sensitivity.

6- Stability: - The ability of a measuring instrument to retain its calibration over a long period of time. Stability determines an instrument's consistency over time.

7- Sensitivity: - a measure of the smallest signal the instrument can measure. Usually, this is defined at the lowest range setting of the instrument

8- Tolerance: - The unwanted but acceptable deviation from a desired dimension.

9- Calibration: - The comparison of a device with unknown accuracy to a device with a known, accurate standard to eliminate any variation in the device is being checked.

Sensors are used in everyday objects such as touch-sensitive elevator buttons (tactile sensor) and lamps which dim or brighten by touching the base. There are also innumerable applications for

sensors of which most people are never aware. Applications include cars, machines, aerospace, medicine, manufacturing and robotics.

4.2.2 Piezoelectricity:

Is the electric charge that accumulates in certain solid materials (such as crystals, certain ceramics, and biological matter such as bone, DNA and various proteins) in response to applied mechanical stress. The word piezoelectricity means electricity resulting from pressure. It is derived from the Greek piezo or piezein which means to squeeze or press, and electric or electron which stands for amber, an ancient source of electric charge .Piezoelectricity was discovered in 1880 by French physicists Jacques and Pierre Curie.

The piezoelectric effect is electromechanical interaction between the mechanical and the electrical state in crystalline materials with no inversion symmetry. The piezoelectric effect is a reversible process in that materials exhibiting the direct piezoelectric effect (the internal generation of electrical charge resulting from an applied mechanical force) also exhibit the reverse piezoelectric effect (the internal generation of a mechanical strain resulting from an applied electrical field). For example, lead zircon ate titan ate crystals will generate measurable piezoelectricity when their static structure is deformed by about 0.1% of the original dimension. Conversely, those same crystals will change about 0.1% of their static dimension when an external electric field is applied to the material. The inverse piezoelectric effect is used in production of

ultrasonic sound waves. (Gautschi, G (2002). Piezoelectric Sensorics: Force, Strain, Pressure, Acceleration and Acoustic Emission Sensors, Materials and Amplifiers.Springer Berlin, Heidelberg, New York.)

4.2.2.1 Sensing materials:

Two main groups of materials are used for piezoelectric sensors: piezoelectric ceramics and single crystal materials.

The ceramic materials (such as PZT ceramic) have a piezoelectric constant / sensitivity that is roughly two orders of magnitude higher than those of the natural single crystal materials and can be produced by inexpensive sintering processes. The piezoeffect in piezoceramics is "trained", so unfortunately their high sensitivity degrades over time. The degradation is highly correlated with temperature. The less sensitive 'natural' single crystal materials (gallium phosphate, quartz, and tourmaline) have a much higher – when carefully handled, almost infinite – long term stability. There are also new single crystal materials commercially available such as Lead Magnesium Niobate-Lead Titan ate (PMN-PT). These materials offer greatly improved sensitivity (compared with PZT) but suffer from a lower maximum operating temperature and are currently much more expensive to manufacture.Piezoelectricity is found in useful applications such as the production and detection of sound, generation of high voltages, electronic frequency generation, microbalances, and ultrafine focusing of optical assemblies.

It is also the basis of a number of scientific instrumental techniques with atomic resolution, the scanning probe micros

copies such as STM, AFM, MTA, SNOM, etc., and everyday uses such as acting as the ignition source for cigarette lighters and push-start.

The principle of operation of a piezoelectric sensor is that a physical dimension, transformed into a force, acts on two opposing faces of the sensing element. Depending on the design of a sensor, different "modes" to load the piezoelectric element can be used: longitudinal, transversal and shear.

A piezoelectric disk generates a voltage when deformed (change in shape is greatly exaggerated).**Figure (4.2).**

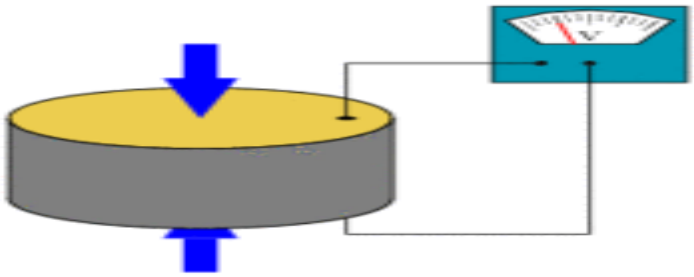

Figure (4.2). A schematic diagram which shows a sample of piezoelectric material (gray) being subject to stress (arrows); the resultant voltage is registered on the volt meter.

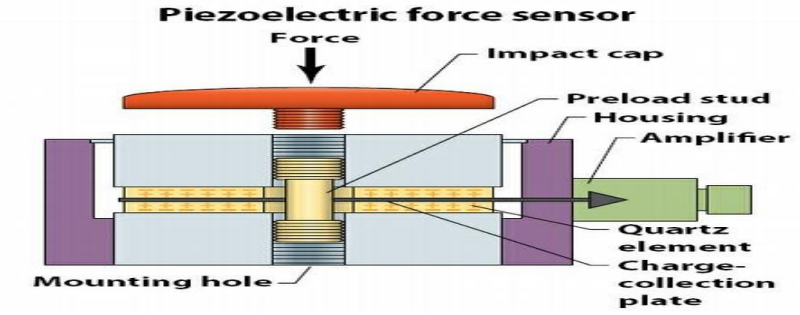

Figure (4.3). This cross-section diagram of a Series 208 Quartz Force Sensor from PCB Piezotronics Inc. of Depew, N.Y., shows the basic assembly of a piezoelectric sensor.

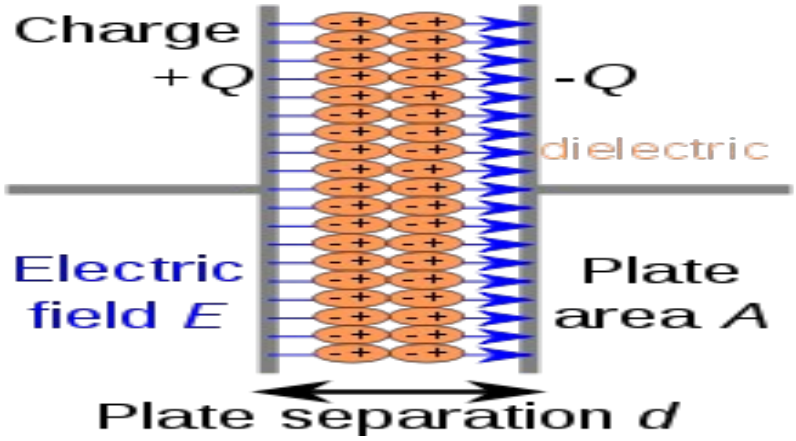

Figure (4.4). Any spatially separated charge will result in an [electric field](), and therefore an [electric potential](). Shown here is a standard dielectric in a [capacitor]().

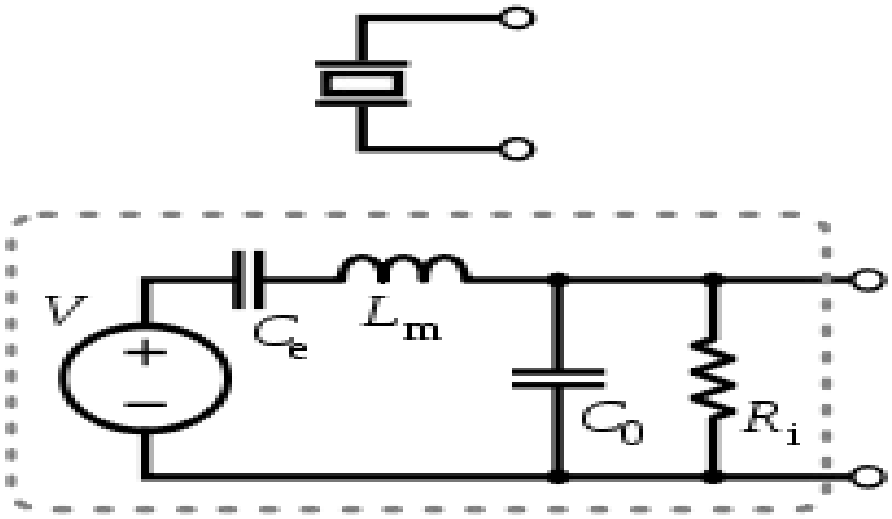

Figure (4.5) Schematic symbol and electronic model of a piezoelectric sensor.

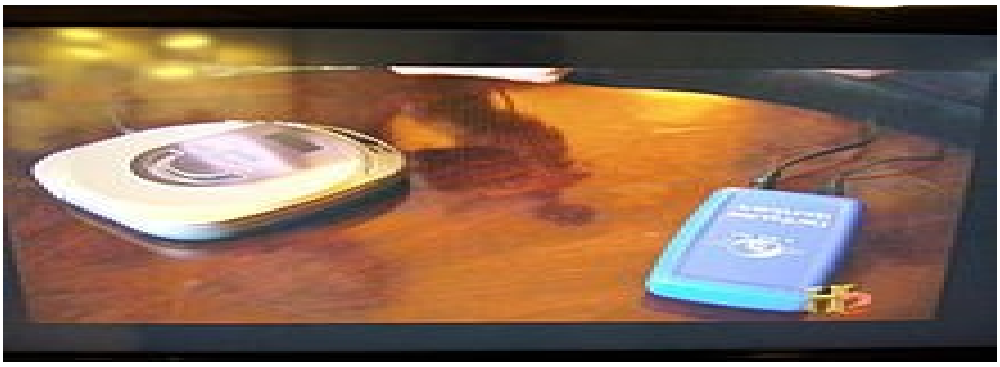

Figure (4.6) A piezoelectric system (Without contact tabs).

4.2.2.2 Electrical properties:

A piezoelectric transducer has very high DC output impedance and can be modeled as a proportional voltage source and filter network. The voltage V at the source is directly proportional to the applied force, pressure, or strain. The output signal is then related to this mechanical force as if it had passed through the equivalent circuit.The piezoelectric properties of quartz are useful as standard of frequency generator (Crystal Oscillator).

4.2.2.3 Applications:

Piezoelectric materials have been used in a wide range of applications including quartz watches, solid state gas lighters, medical ultrasound imagers, sound systems, and micro fluidic pumps, and some other applications, such as in medical, aerospace, nuclear instrumentation, and as a pressure sensor in the touch pads of mobile phones.

4.2.2.4 Integrated Silicon Pressure Sensor:

MPX4115A/MPXA4115A series sensor integrates on–chip, bipolar op amp circuitry and thin film resistor networks to provide a high output signal and temperature compensation. The small form factor and high reliability of on–chip integration make the pressure sensor a logical and economical choice for the system designer.

The MPX4115A/MPXA4115A series piezoresistive transducer is a state–of–the–art, monolithic, signal conditioned, silicon pressure sensor. This sensor combines advanced micromachining techniques, thin film metallization, and bipolar semiconductor processing to provide an accurate, high level analog output signal that is proportional to applied pressure.

4.2.2.5 Features:

1- 1.5% Maximum Error over 0° to 85°C

2- Ideally suited for Microprocessor or Microcontroller–Based Systems

3- Temperature Compensated from –40° to +125°C.

4- Durable Epoxy Unibody Element or Thermoplastic
(PPS) Surface Mount Package.

4.2.2.6 Application Examples:

1- Industrial Controls.

2- Engine Control.

3- Weather Stations and Weather Reporting Devices.

High reliability of on-chip integration makes the Free scale BAP sensor a logical
And economical choice for application designers.

4.3 preamplifier:

A preamplifier (preamp) is an electronic amplifier that prepares a small electrical signal for further amplification or processing. A preamplifier is often placed close to the sensor to reduce the effects of noise and interference. It is used to boost the signal strength to drive the cable to the main instrument without significantly degrading the signal-to-noise ratio (SNR). The noise performance of a preamplifier is critical, when the gain of the preamplifier is high; the SNR of the final signal is determined by the SNR of the input signal and the noise figure of the preamplifier.

4.3.1 Low-noise amplifiers (LNA):

Is an electronic amplifier used to amplify possibly very weak signals (for example, captured by an antenna). It is usually located very close to the detection device to reduce losses in the feed line.

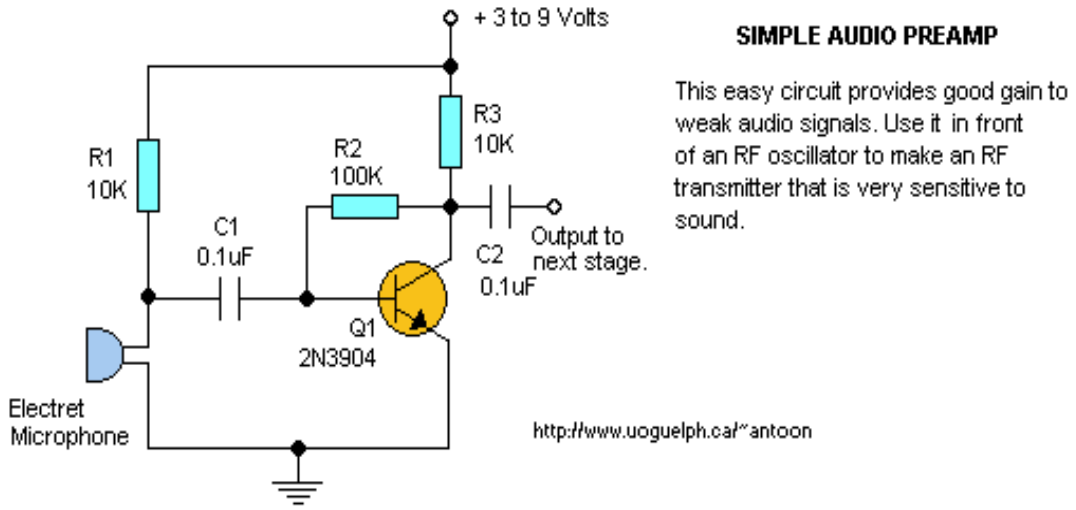

Figure (4.7) Simple audio preamplifier (single stage) .

4.4 Signal Conditioning:

In electronics, signal conditioning means manipulating an analog signal in such a way that it meets the requirements of the next stage for further processing. Most common use is in analog-to-digital converters.

In control engineering applications, it is common to have a sensing stage (which consists of a sensor), a signal conditioning stage (where usually amplification of the signal is done) and a processing stage (normally carried out by an ADC and a micro-controller). Operational amplifiers (op-amps) are commonly employed to carry out the amplification of the signal in the signal conditioning stage.Signal inputs accepted by signal conditioners include DC voltage and current, AC voltage and current, frequency and electric charge. Sensor inputs can be accelerometer, thermocouple, thermistor, resistance thermometer, strain gauge, pressure sensor or bridge, and LVDT or RVDT. Specialized inputs include encoder, counter or tachometer, timer or clock, relay or switch, and other specialized inputs. Outputs for signal conditioning equipment can be voltage, current, frequency, timer or counter, relay, resistance or potentiometer, and other specialized outputs.

Signal conditioning can include amplification, filtering, converting, range matching, isolation and any other processes required to make sensor output suitable for processing after conditioning.

Filtering is the most common signal conditioning function, as usually not all the signal frequency spectrum contains valid data.

Signal amplification performs two important functions: increases the resolution of the inputed signal, and increases its signal-to-noise ratio. For example, the output of an electronic temperature sensor, which is probably in the millivolts range is probably too low for an Analog-to-digital converter (ADC) to process directly. In this case it is necessary to bring the voltage level up to that required by the ADC.

Magnetic or optic isolation can be used. Magnetic isolation transforms the signal from voltage to a magnetic field, allowing the signal to be transmitted without a physical connection (for example, using a transformer). Optic isolation takes an electronic signal and modulates it to a signal coded by light transmission (optical encoding), which is then used for input for the next stage of processing.

It is primarily utilized for data acquisition, in which sensor signals must be normalized and filtered to levels suitable for analog-to-digital conversion so they can be read by computerized devices. Other uses include preprocessing signals in order to reduce computing time, converting ranged data to boolean values, for example when knowing when a sensor has reached certain value..

4.5 Analogue to digital convertor (ADC):

An analog-to-digital converter (abbreviated ADC, A/D or A to D) is a device that converts a continuous physical quantity (usually voltage) to a digital number that represents the quantity's amplitude.

On the other hand A/D converters are electrical circuits that have the following characteristics.

1- The input to the A/D converter is a voltage.

2- A/D converters may be designed for voltages from 0 to 10v, from -5 to +5v, etc., but they almost always take a voltage input. (Some rare exceptions occur with current inputs!) In any event, the input is an analog voltage signal for most cases.

3- The output of the A/D converter is a binary signal, and that binary signal encodes the analog input voltage. So, the output is some sort of digital number.

An ADC often performs the conversions ("samples" the input) periodically. The result is a sequence of digital values that have converted a continuous-time and continuous-amplitude analog signal to a discrete-time and discrete-amplitude digital signal.

Electrical Symbol for analogue to digital convertor seen in **Figure (4.9)** .

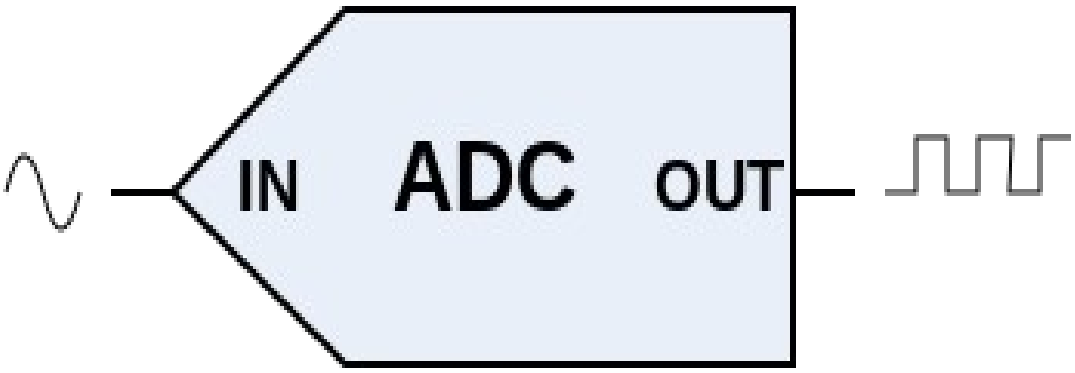

Figure (4.8) ADC symbol.

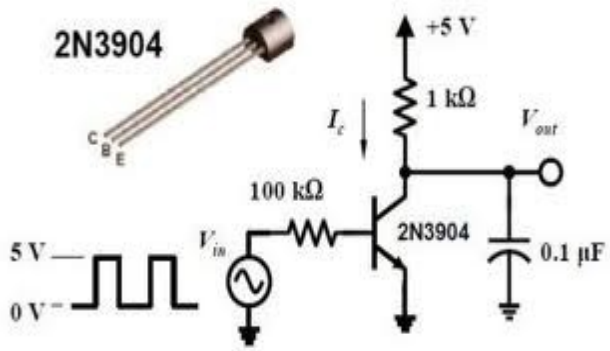

Figure (4.9) ADC using transistor as switch .

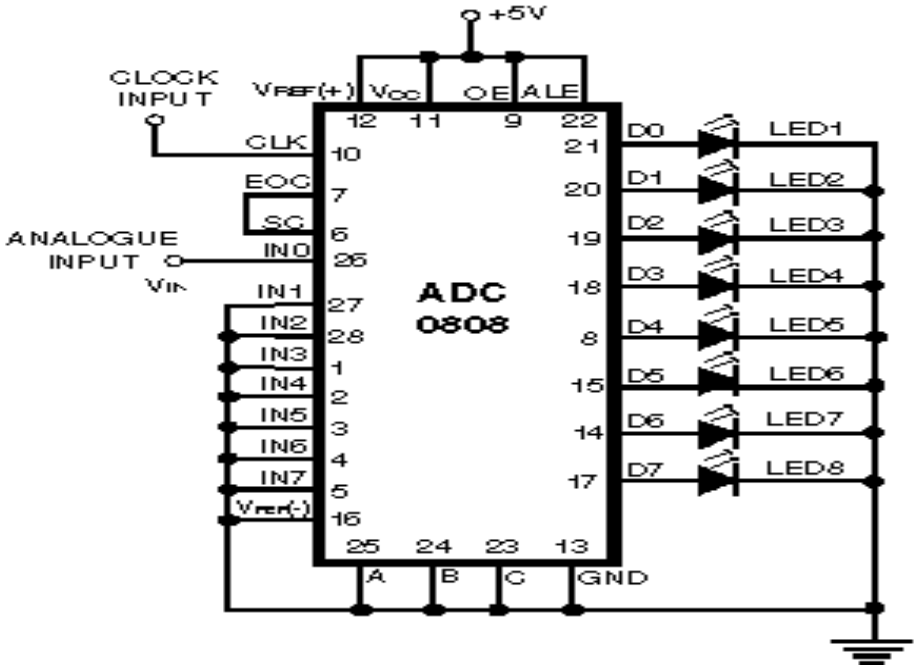

Figure (4.10) ADC chip .

4.6 An operational amplifier:

An operational amplifier (op-amp) is a DC-coupled high-gain electronic voltage amplifier with a differential input and, usually, a single-ended output. In this configuration, an op-amp produces

an output potential (relative to circuit ground) that is typically hundreds of thousands of times larger than the potential difference between its input terminals.

Operational amplifiers had their origins in analog computers, where they were used to do mathematical operations in many linear, non-linear and frequency-dependent circuits. Characteristics of a circuit using an op-amp are set by external components with little dependence on temperature changes or manufacturing variations in the op-amp itself, which makes op-amps popular building blocks for circuit design.

Op-amps are among the most widely used electronic devices today, being used in a vast array of consumer, industrial, and scientific devices.

4.6.1 Circuit notation:

The circuit symbol for an op-amp is shown in Figure(3.12) where:

1- V+: non-inverting input

2- V−: inverting input

3- Vout: output

4- VS+: positive power supply

5- VS−: negative power supply

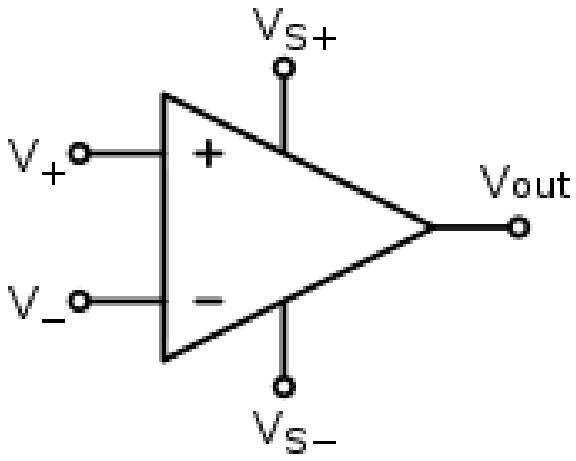

Figure (4.11) Circuit diagram symbol for an op-amp

The power supply pins (VS+ and VS−) can be labeled in different ways (See IC power supply pins). Often these pins are left out of the diagram for clarity, and the power configuration is described or assumed from the circuit.

4.6.2 Op-amp characteristics:

4.6.2.1 Ideal Op-amps:

An ideal op-amp is usually considered to have the following properties:

1- Infinite open-loop gain

2- Infinite voltage range available at the output

3- Infinite bandwidth with zero phase shift and infinite slew rate

4- Infinite input impedance and so zero input current and zero input offset voltage

5- Zero output impedance

6- Zero noise

7- Infinite Common-mode rejection ratio (CMRR)

8- Infinite Power supply rejection ratio.

Non ideal operational amplifier equivalent circuit seen in **Fig. (3.13**) Bellow:

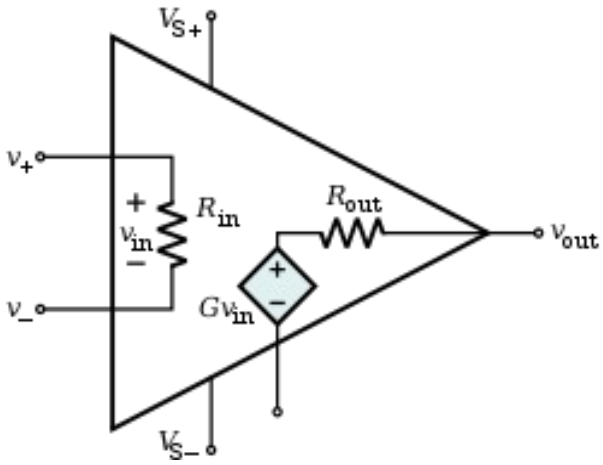

Figure (4.12) An equivalent circuit of an operational amplifier that models some resistive non-ideal parameters.

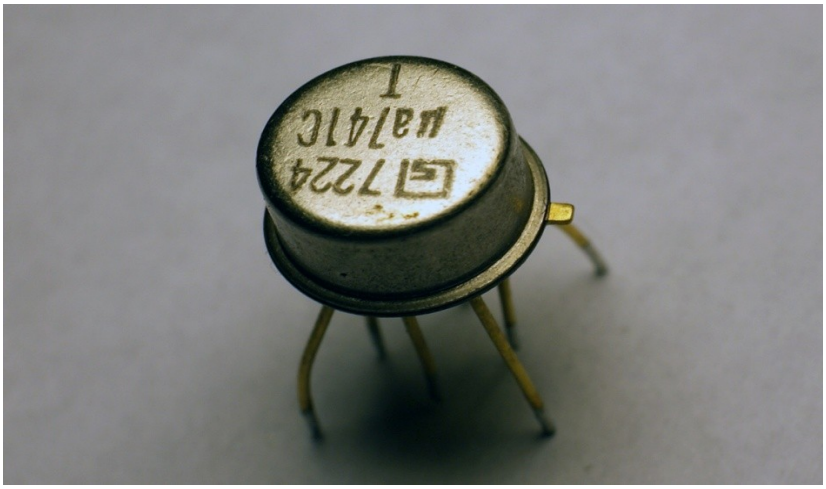

Figure (4.13) A Signetics µa741 operational amplifier, one of the most successful op-amps.

Internal circuitry of 741 type op-amp seen in **Figure (4.14)** bellow:

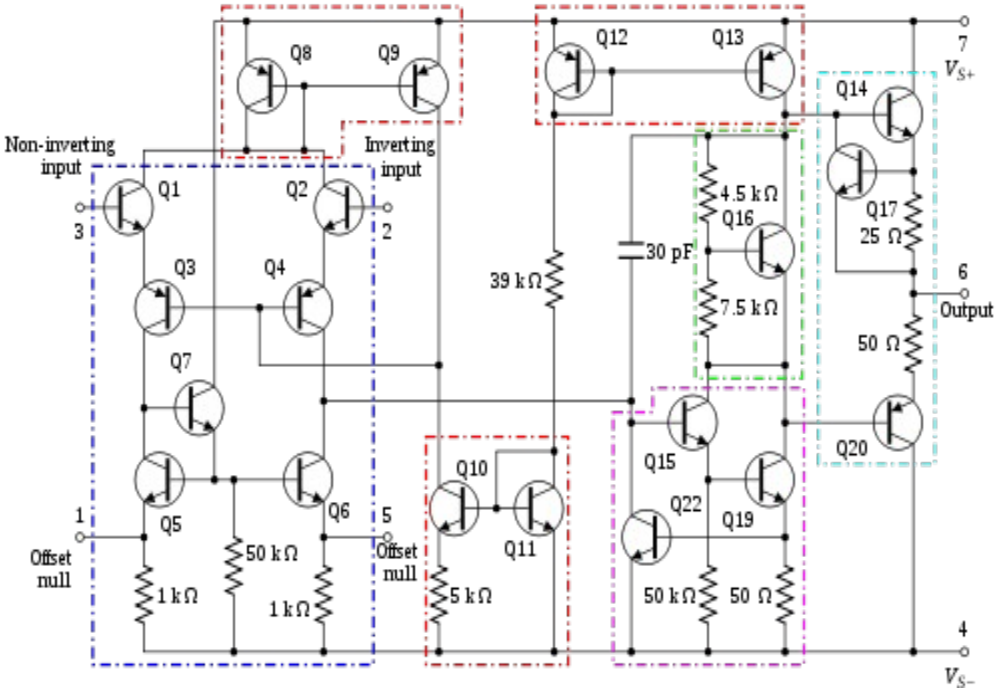

Figure (4.14) A component level diagram of the common 741 op-amp.

Though designs vary between products and manufacturers, all op-amps have basically the same internal structure, which consists of three stages:

1. Differential amplifier — provides low noise amplification, high input impedance, usually a differential output.
2. Voltage amplifier — provides high voltage gain, a single-pole frequency roll-off, usually single-ended output.

3. Output amplifier — provides high current driving capability, low output impedance, current limiting and short circuit protection circuitry.

4.7 Microcontroller:

A microcontroller is the type of small computer on a single integrated circuit. Which contains a processor core, programmable Input/ Output and Memory (Ram/Rom) and Timers. A microcontroller (sometimes abbreviated µC, uC or MCU).

Microcontrollers are designed for embedded applications, in contrast to the microprocessors used in personal computers or other general purpose applications.

Microcontrollers are used in automatically controlled products and devices, such as automobile engine control systems, implantable medical devices, remote controls, office machines, appliances, power tools, toys and other embedded systems.

There are different types and applications as per their capability and feasibility to perform the desired task, most common of these are 8051, AVR and PIC microcontrollers. Microcontrollers are used in a wide number of electronic systems such as :

1- Counters .

2- Control systems in industries .

3- Mobile phones.

4- Security systems.

5- Hearing aids.

6- TV, Radio, CD players.

4.7.1 At mega 16 Microcontroller:

The AVR is a modified Harvard architecture 8-bit RISC single chip microcontroller which was developed by Atmel in 1996. The AVR was one of the first microcontroller families to use on-chip flash memory for program storage, as opposed to one-time programmable ROM, EPROM, or EEPROM used by other microcontrollers at the time. AVR stands for Alf (Egil Bogen) and Vegard (Wollan)'s RISC processor. also known as Advanced Virtual RISC.

This chip represent one of good and reliable microcontrollers family, where

AT refers to the manufacturer Atmel, Mega means that the microcontroller belong to Mega AVR category, 16 signifies the memory of the controller, which is 16KB.

4.7.2 Features of At mega 16:

1- **16KB of** Flash memory
2- 1KB of SRAM
3- 512 Bytes of EEPROM
4- Available in 40-Pin DIP
5- 8-Channel 10-bit ADC
6- Two 8-bit Timers/Counters
7- One 16-bit Timer/Counter
8- 4 PWM Channels
9- In System Programmer (ISP)
10-Serial USART
11-SPI Interface
12-Digital to Analog Comparator.

Figure (4.15)2 ATmega16 micro controllers

ttp://www.engineersgarage.com/electronic-components/atmega16-microcontr. 2012 EngineersGarage.

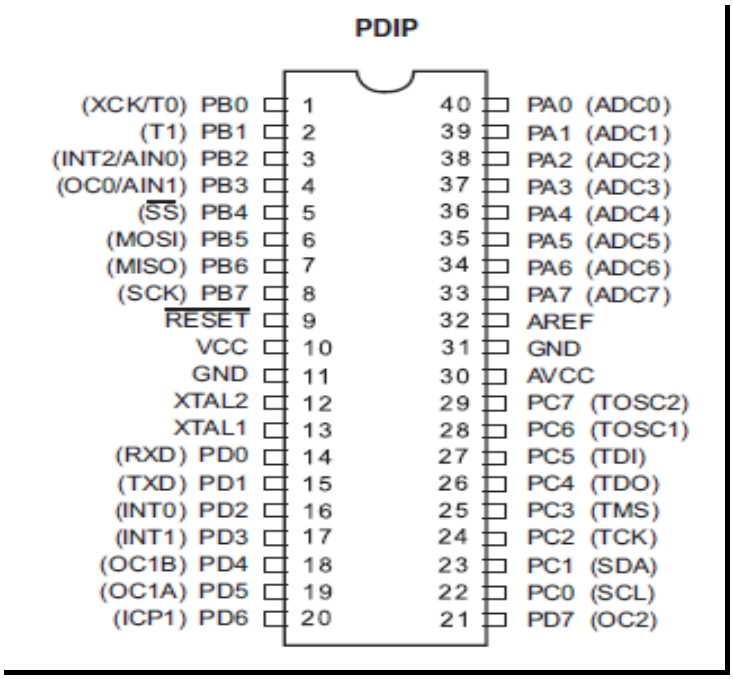

Figure(4.16): PIN description of Atmega16

Table(4.1) Used pin description:

Pin No.	Pin name	Description	Alternate Function
1	(XCK/T0) PB0	I/O PORTB, Pin	T0: Timer0 External Counter Input.

			XCK : USART External Clock
2	(T1) PB1	I/O PORTB, Pin	I/O T1:Timer1 External Counter Input
9	RESET	Reset Pin, Active Low Reset	
10	Vcc	Vcc = +5V	
11	GND	GROUND	
14	(RXD) PD0	I/O PORTD, Pin	USART Serial Communication Interface
15	(TXD) PD1	I/O PORTD, Pin	
16	(INT0) PD2	I/O PORTD, Pin	External Interrupt INT0
17	(INT1) PD3	I/O PORTD, Pin	External Interrupt INT1
18	(OC1B) PD4	I/O PORTD, Pin	PWM Channel Outputs
21	PD7 (OC2)	I/O PORTD, Pin	Timer/Counter2 Output Compare Match Output
22	PC0 (SCL)	I/O PORTC, Pin	TWI Interface
23	PC1 (SDA)	I/O PORTC, Pin	
24	PC2 (TCK)	I/O PORTC, Pin	JTAG Interface
26	PC4 (TDO)	I/O PORTC, Pin	
27	PC5 (TDI)	I/O PORTC, Pin	
28	PC6 (TOSC1)	I/O PORTC, Pin	Timer Oscillator Pin 1
29	PC7 (TOSC2)	I/O PORTC, Pin	Timer Oscillator Pin 2

30	AVcc	Voltage Supply = Vcc for ADC	
31	GND	GROUND	
32	AREF	Analog Reference Pin for ADC	
37	PA3	I/O PORTA,	ADC Channel 3
	(ADC3)	Pin	
38	PA2	I/O PORTA,	ADC Channel 2
	(ADC2)	Pin	
39	PA1	I/O PORTA,	ADC Channel 1
	(ADC1)	Pin	
40	PA0	I/O PORTA,	ADC Channel 0
	(ADC0)	Pin	

4.7.3 Programming environments:

Microcontrollers were originally programmed only in assembly language, but various high-level programming languages are now also in common use to target microcontrollers. These languages are either designed specially for the purpose, or versions of general purpose languages such as the C programming language. Typically microcontroller programs must fit in the available on-chip program memory, since it would be costly to provide a system with external, expandable, memory. Compilers and assemblers are used to convert high-level language and assembler language codes into a compact machine code for

storage in the microcontroller's memory. Depending on the device, the program memory may be permanent, read-only memory that can only be programmed at the factory, or program memory that may be field-alterable flash or erasable read-only memory.The Code vision is the program used in this project to simulate circuit operation.

4.8 Driver:

In electronics, a driver is an electrical circuit or other electronic component used to control another circuit or other component, such as a high-power transistor.

4.8.1 ULN 2003A :

The ULN2003A is a monolithic IC consists of seven NPN Darlington transistor pairs voltage and current capability. It is commonly used for applications such as relay drivers, motor, display drivers, led lamp drivers, logic buffers, line drivers, hammer drivers and other high voltage current applications. It consists of common cathode clamp diodes for each NPN Darlington pair which makes this driver IC useful for switching inductive loads (https://www.google.com/Ligo George. electrosome.com/uln2003-high-voltage-current-driver/ - Feb 24, 2013)**. Fig.(4.18)** shows a picture of ULN 2003A driver bellow:

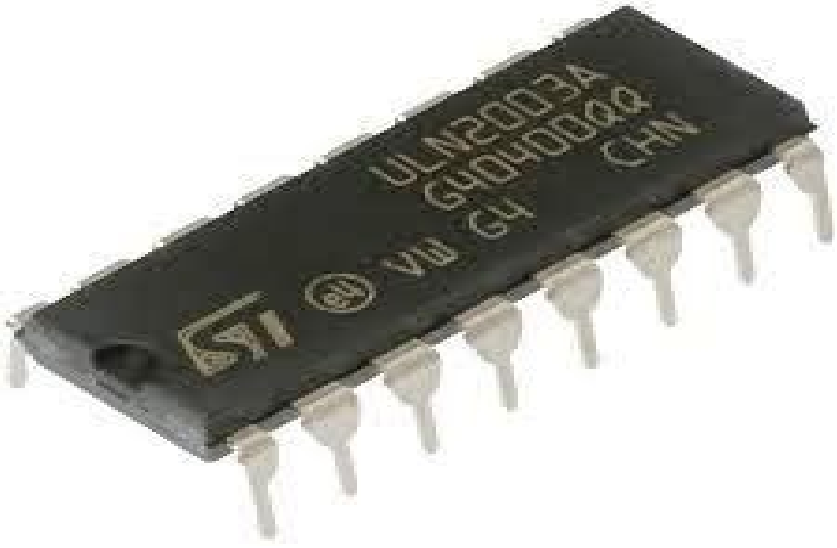

Fig.(4.17) ULN 2003A

The output of the driver is open collector and the collector current rating of each Darlington pair is 500mA. Darlington pairs may be paralleled if higher current is required. The driver IC also consists of a 2.7KΩ base resistor for each Darlington pair. Thus each Darlington pair can be operated directly with TTL or 5V CMOS devices. This driver IC can be used for high voltage applications up to 50V.

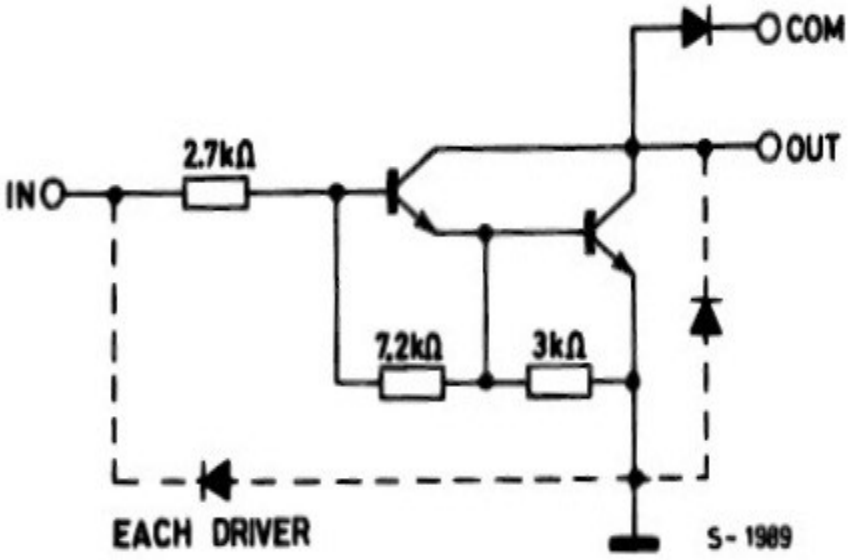

Figure (4.18) Schematic Diagram of each Darlington Pair – ULN2003.

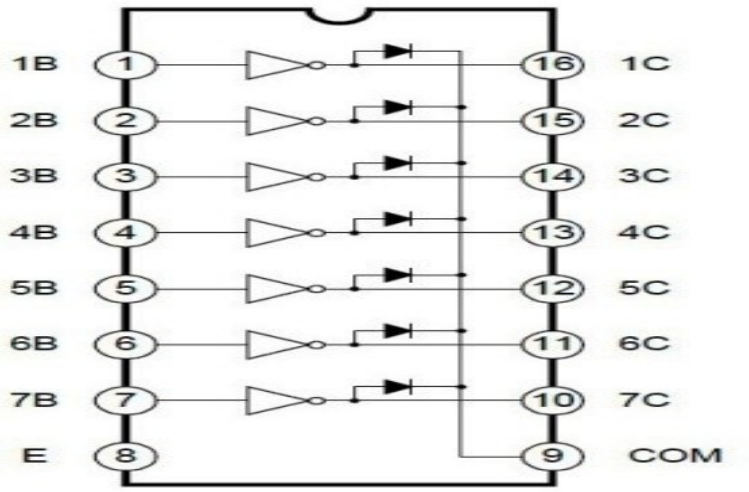

Figure (4.19) Logic Diagram of ULN2003

Note that the driver provides open collector output, so it can only sink current, cannot source. Thus when a 5V is given to 1B terminal, 1C terminal will be connected to ground via Darlington pair and the maximum current that it can handle is 500A. From the above logic diagram we can see that cathode of protection diodes are shorted to 9th pin called COM. So for driving inductive loads, it must connected to the supply voltage.ULN2003 is widely used in relay driving and stepper motor driving applications.

4.9 Stepper motor:

A stepper motor is an electromechanical device which converts electrical pulses into discrete mechanical movements. The shaft or spindle of a stepper motor rotates in discrete step increments when electrical command pulses are applied to it in the proper sequence. The motors rotation has several direct relationships to these applied input pulses. The sequence of the applied pulses is directly related to the direction of motor shafts rotation. The speed of the motor shafts rotation is directly related to the frequency of the input pulses and the length of rotation is directly related to the number of input pulses applied. The movement readed by each pulse is precise and repeatable, which is why stepper motors are so effective for positioning applications. Stepper motors are an excellent solution for applications such as machine control, manufacturing test, semiconductor positioning, biomedical machines, and lab automation.

4.9.1 Stepper Motor Theory of Operation:

Stepper motors provide a means for precise positioning and speed control without the use of feedback sensors. The basic operation of a stepper motor allows the shaft to move a precise number of degrees each time a pulse of electricity is sent to the motor. Since the shaft of the motor moves only the number of degrees that it was designed for when each pulse is delivered, you can control the pulses that are sent and control the positioning and speed. The rotor of the motor produces torque from the interaction between the magnetic field in the stator and rotor. The strength of the magnetic fields is proportional to the amount of current sent to the stator and the number of turns in the windings.

The stepper motor uses the theory of operation for magnets to make the motor shaft turn a precise distance when a pulse of electricity is provided. Depending on the fact that, like poles of a magnet repel and unlike

Poles attract. **Figure (4.20):**

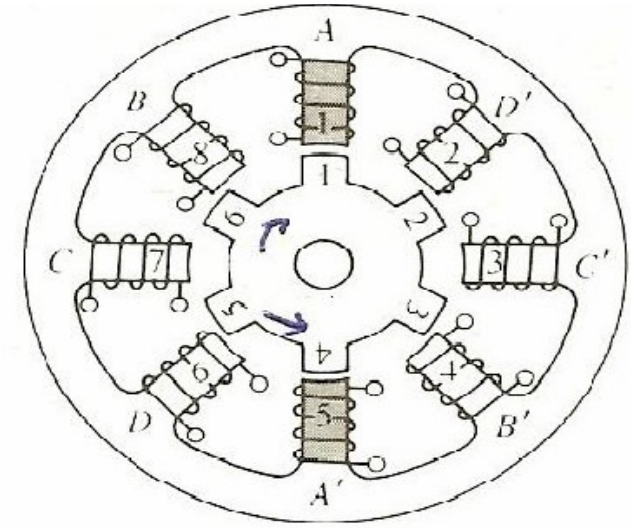

Figure (4.20) Diagram that shows the position of the six-pole rotor

and eight-pole stator of a typical stepper motor.

Shows a typical cross-sectional view of the rotor and stator of a stepper motor. From this diagram you can see that the stator (stationary winding) has eight poles, and the rotor has six poles (three complete magnets). The rotor will require 24 pulses of electricity to move the 24 steps to make one complete revolution. Another way to say this is that the rotor will move precisely 15° for each pulse of electricity that the motor receives. The number of degrees the rotor will turn when a pulse of electricity is delivered to the motor can be calculated by dividing the number of degrees in one revolution of the shaft(360°) by the number of poles (north and south) in the rotor. In this stepper motor 360° is divided by 24 to get 15°. When no power is applied to the motor, the residual magnetism in the rotor magnets will cause the rotor to detent or align one set of its magnetic poles with the magnetic poles of one of the stator magnets. This means that the rotor will have 24 possible detent positions. When the rotor is in a detent position, it will have enough magnetic force to keep the shaft from moving to the next position.

This is what makes the rotor feel like it is clicking from one position to the next as you rotate the rotor by hand with no power applied.

4.9.2 Some properties of stepper motors :

1- Stepper motors are operated open loop.

2- Stepper motors are easily controlled with microprocessors; however logic and drive electronics are more complex.

3-Stepper motors are brushless and brushes contribute several problems, e.g., wear, sparks, electrical transients.

4-DC motors have a continuous displacement and can be accurately positioned, whereas stepper motor motion is incremental and its resolution is limited to the step size.

5-Stepper motors can slip if overloaded and the error can go undetected. (A few stepper motors use closed-loop control.)

7- Feedback control with DC motors gives a much faster response time.

4.9.3 Stepper Motor Advantages and Disadvantages:

4.9.3.1 Advantages:

1. A step angle of the motor is proportional to the input pulse.
2. The motor has full torque at standstill (if the windings are energized).
3. Precise positioning and repeatability of movement since good stepper motors have an accuracy of 3 – 5% of a step and this error is non cumulative from one step to the next.
4. Excellent response to starting/stopping/reversing.
5. Very reliable since there are no contact brushes in the motor. Therefore the life of the motor is simply dependant on the life of the bearing.
6. The motors response to digital input pulses provides open-loop Control, making the motor simpler and less costly to control.
7. It is possible to achieve very low speed synchronous rotation with a Load that is directly coupled to the shaft.

8. A wide range of rotational speeds can be realized as the speed is proportional to the frequency of the input pulses.

4.9.3.2 Disadvantages of stepper motor:

1-They have low torque capacity (typically less than 2,000 oz-in) compared to DC motors.

2-They have limited speed (limited by torque capacity and by pulse-missing problems due to fully switching systems and drive circuits).

3-They have high vibration levels due to stepwise motion

4-Large errors and oscillations can result when a pulse is missed under open-Loop control.

4.10 Regulated power supply:

A regulated power supply is an embedded circuit; it converts unregulated AC into a constant DC. With the help of a rectifier it converts AC supply into DC. Its function is to supply a stable voltage (or less often current), to a circuit or device that must be operated within certain power supply limits. The output from the regulated power supply may be alternating or unidirectional, but is nearly always DC (Direct Current

The type of stabilization used may be restricted to ensuring that the output remains within certain limits under various load conditions, or it may also include compensation for variations in its own supply source. The latter is much more common today.

4.10.1 Voltage regulator:

A voltage regulator is designed to automatically maintain a constant voltage level. A voltage regulator may be a simple "feed-forward" design or may include negative feedback control

loops. It may use an electromechanical mechanism, or electronic components. Depending on the design, it may be used to regulate one or more AC or DC voltages, **Fig.(3.21)** Voltage regulator IC as shown:

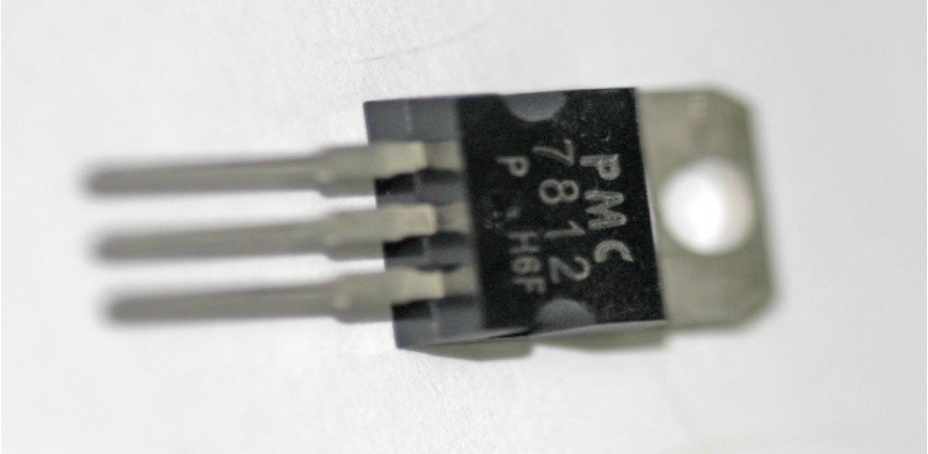

Figure (4.21) A popular three pin +12 V DC voltage regulator IC.

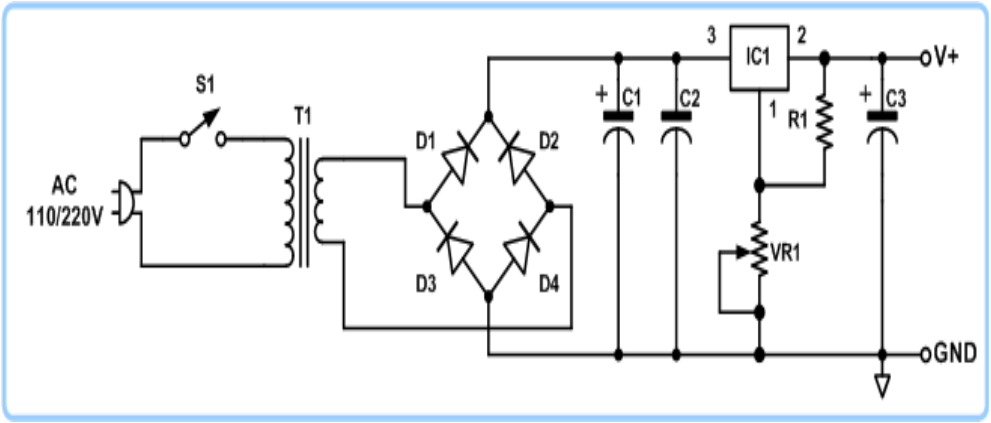

Figure(4.22) Regulated DC voltage circuit diagram.

Electronic voltage regulators are found in devices such as computer power supplies where they stabilize the DC voltages used by the processor and other elements. In automobile alternators and central power station generator plants, voltage

regulators control the output of the plant. In an electric power distribution

system, voltage regulators may be installed at a substation or along distribution lines so that all customers receive steady voltage independent of how much power is drawn from the line.

4.10.2 Applications:

1- D.C. variable bench supply (a bench power supply usually refers to a power supply capable of supplying a variety of output voltages useful for bench testing electronic circuits, possibly with continuous variation of the output voltage, or just some preset voltages; a laboratory (lab) power supply normally implies an accurate bench power supply, while a balanced or tracking power supply refers to twin supplies for use when a circuit requires both positive and negative supply rails).

2- Mobile Phone power adaptors.

3- Regulated power supplies in appliances.

4- Various amplifiers and oscillators.

4.11 Gear Ratio:

Considering gear (A) as the one of the stepper motor and gear (B) is to be directly coupled to it as shown in Figure (4.23) so as to increase the torque and reduce the speed , as we interest in torque rather than speed.

Gear (B) is useful to increase the accuracy of positioning i.e. if the stepper is chosen as 60 for step that will be transferred to the collimator pane through gear (B) as 6/3= (20). If the panel is directly coupled to the stepper it will move (60) each step, while with gear(B) the move will be only (20) which is more precise.

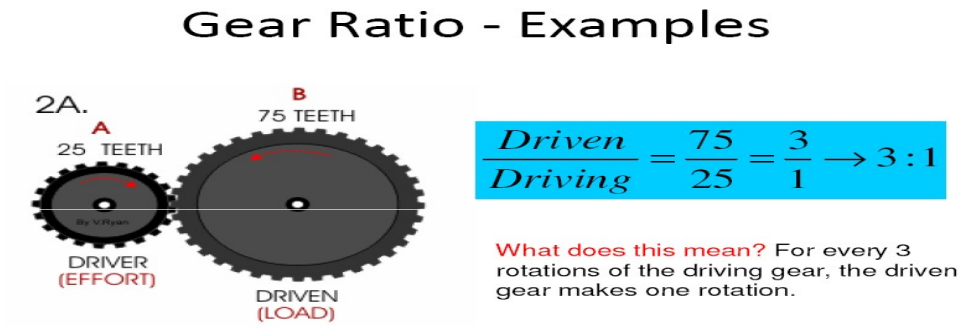

Figure (4.23) Gear box ratio

Chapter Five

Proposed Solution(Methodology)

5.1 **System Construction:**

The adaptive control system is mainly constructed from pressure sensor, signal conditioning, analog to digital converter (ADC), Microcontroller (Atmega-16), driver circuit and stepper motor in addition to regulated DC power supply for biasing purpose as shown in block diagram figure (5.1).

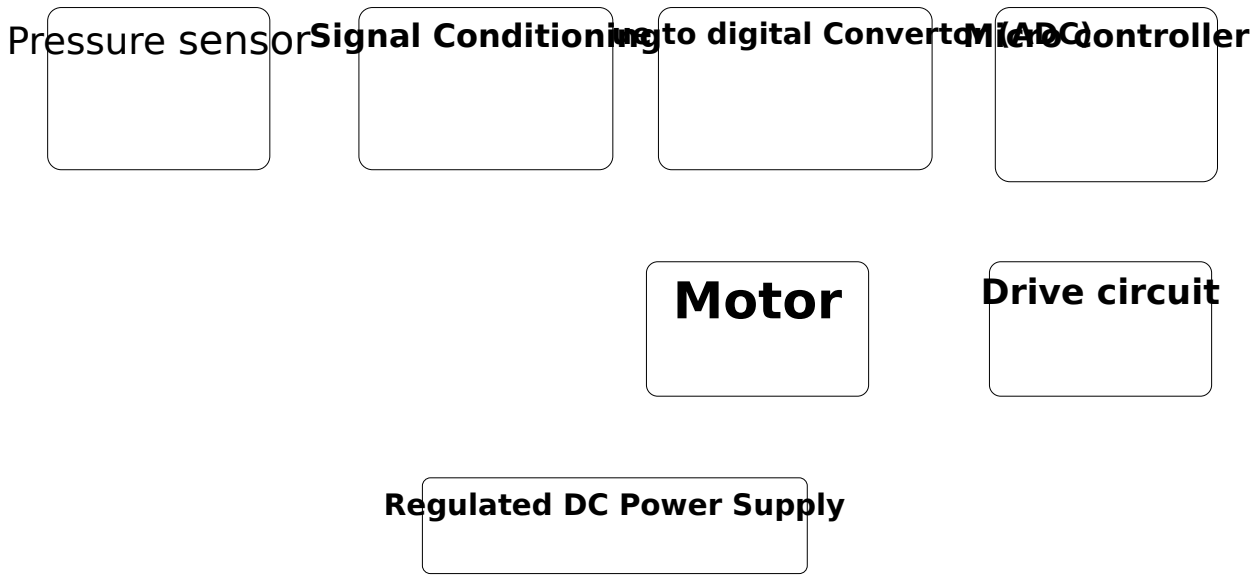

Figure (5.1) System block diagram.

5.2 List of components:

1. Pressure sensor (MPX4250)
2. MCU (at mega 16L).
3. Drivers (ULN2003A).
4. Stepper motors .
5. Set of mechanical gears.
6. Battery of 12V.
7. Regulator 5V (7805).

5.3 General Operation View:

First of all, the pressure sensor attached to the chest or abdomen wall of a volunteered person in a normal breathing rate (0.5Hz), then the pressure sensor sense the mechanical movement (Physiological Motion) of the abdomen due to breathing (inspiration expiration).

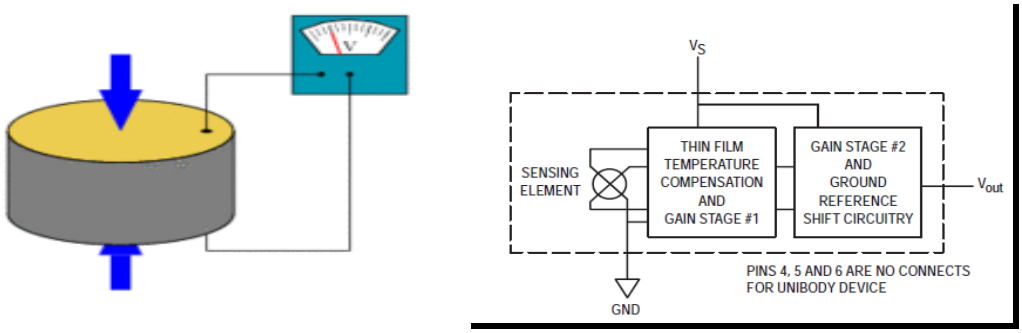

Figure (5.2)Outer and Internal construction stages of the integrated silicon pressure sensor MPX4250, response up to 250 Kpa to generate 5 V as maximum.

As a result the pressure of the abdomen will translate into positive electrical analog signal having small value and may be distorted depending upon the patient pressure value (Kpa), that is to say, the greater abdomen pressure the greater positive generated out put voltage, the generated voltage during inhalation increases from zero (0) volt up to about 5 volts as maximum and the correlation between breathing pressure and the generated volts shows the following linear equation(1):

$$y = 0.02x + 0.26 \text{ (for inhalation)} \ldots\ldots\ldots\ldots\ldots\ldots (1)$$

Where :

y : Represent the out put voltage (volt).

x: Is the pressure applied(Kpa).

0.26: Is the constant .

So, the calculated out put voltage resulted due to pressure applied(Inhalation state) shown in table(5.1).

Table (5.1) Pressure applied and voltage grow up

Pressure (Kpa)	Voltage Output(V)
0	0.26
20	0.66
40	1.06
60	1.46
80	1.86
100	2.26
120	2.66
140	3.06
160	3.46
180	3.86
200	4.26
220	4.66
240	5.06
250	5.26

While exhalation state (Re pressure from 250 to 0 kpa) is denoted by the following linear equation(2):

$$y = - 0.02x + 0.26 \text{ for (exhalation)} \quad (2)$$

The calculated output voltage resulted due to exhalation state shown in table(5.2):

Table (5.2) Re-pressing pressure sensor and slow down voltage output .

Re-Press pressure (kpa)	Down voltage Output(V)
250	5.26
240	5.06
220	4.66
200	4.26
180	3.86
160	3.46
140	3.06
120	2.66
100	2.26
80	1.86
60	1.46
40	1.06
20	0.66
0	0.26

While the breathing rate is affect in the signal frequency(Hz), that is to say, high breathing rate gives more signal frequency (Not more than 1Hz) and vise versa.

The signal conditioning stage is used for amplification (Operational amplifier) that should be putted near the pressure sensor, low noise and high signal to noise ratio in order to increase the resolution of the signal and signal-to-noise ratio. Such generated voltage signal has been plotted versus breathing

pressure, this makes the signal strong enough to meets the requirements of the next stage for further processing, commonly use in analog-to-digital converters (ADC). Also low pass filtering is used in this stage to cancel any unwanted signals see figure(5.3).

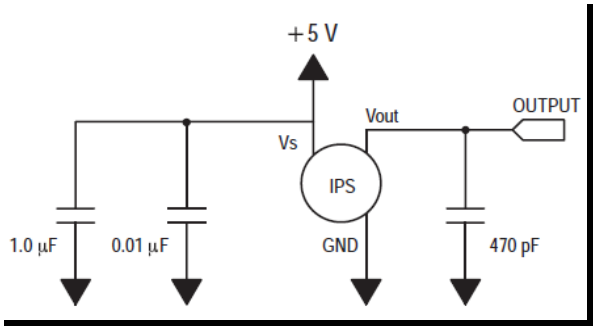

Figure (5.3): Shows the integrated filtering with integrated pressure sensor (IPS).

See figure (5.4) that shows sample pressure out put signal resulted from physiological motion of abdomen affected with breathing condition. The consideration that been considered is the out put all ways positive sine wave shape what ever the case (condition) of breathing, that is to say, the output voltage grows up from zero voltage to maximum(At inhalation state) and from max. to zero(At exhalation state) during breathing duration time.

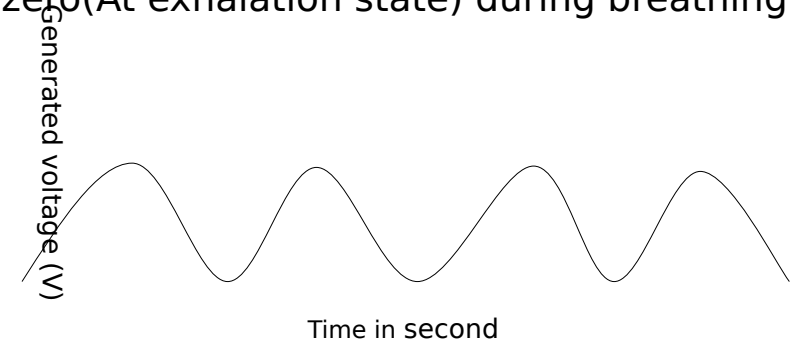

Figure(5.4) Shows the pressure sensor generated signal

The analog to digital converter (ADC) is used to convert the analog signal into digital form (0-1) to make the previous stage able to deal with next stage (microcontroller).

The the microcontroller is been programmed using assembly language .Code vision software program is used to simulate system operation in the way that, the microcontroller generate electrical pulse in sequence of {12,6,3,9} resulting according to the condition bellow see figure(5.5) :

If (current value – Previous value)volt > 0

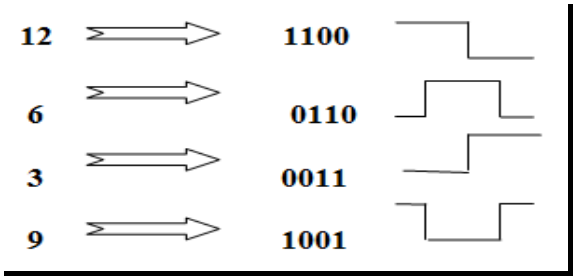

Figure(5.5)Shows analog to digital conversion (Inhalation state)

Repeat the cycle in intervals equal (dt) during Inhalation state duration time.

On the other hand, figure (5.6) shows the microcontroller generate electrical pulse in sequence of {9,3,6,12} resulting according to the condition bellow :

If (current value – Previous value)volt < 0

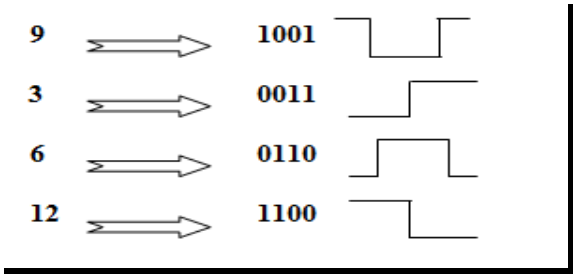

Figure (5.6)shows analog to digital conversion (Exhalation state)

Repeat the cycle in intervals equal (dt) during Exhalation state duration time.

The driver stage is electrical or electronic circuit used to synchronize between the two stages having different power, since microcontroller operating voltage (5v) while the stepper motor work at (12v), so the driver stage acting as if it is buffering amplifier for compatibility purpose and protection (Switch wise) using darling ton pair driver circuit see figure(5.7).

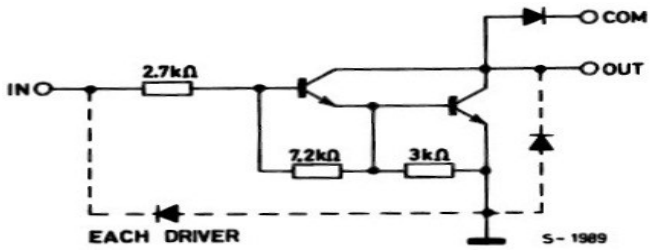

Figure (5.7) Schematic Diagram of each Darlington Pair – ULN2003.

The stepper motor which defined as electromechanical device that convert the electrical pulses into discrete mechanical motion, is used here to receive the electrical pulses that resulted from the abdomen physiological motion during breathing to rotate clock wise at (Inhalation duration time) and anti clock wise at (Exhalation duration time). The shaft or spindle of a stepper motor rotates in discrete step increments when electrical command pulses are applied to it in the proper sequence. The motors rotation has several direct relationships to these applied input pulses. The sequence of the applied pulses is directly related to the direction of motor shafts rotation. The speed of the motor shafts rotation is directly related to the frequency of the

input pulses and the length of rotation is directly related to the number of input pulses applied. The movement readed by each pulse is precise and repeatable; hence the stepper motors are so effective for positioning applications, excellent solution for applications such as machine control, see figure (5.8).

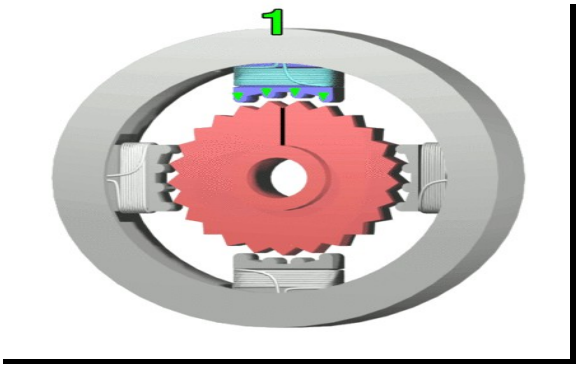

Figure (5.8) Shows the position of the eight-pole rotor and Four -pole stator of a typical stepper motor, the signal initializing the magnet at No. 1

The gear box is used to synchronize motion between the stepper that attached with the primary gear(A), while the collimator axial attached to the secondary gear box(B) to balance the rotation of the stepper motor with the axial collimator ,then gives the desired displacement of the collimator see figure(5.9).

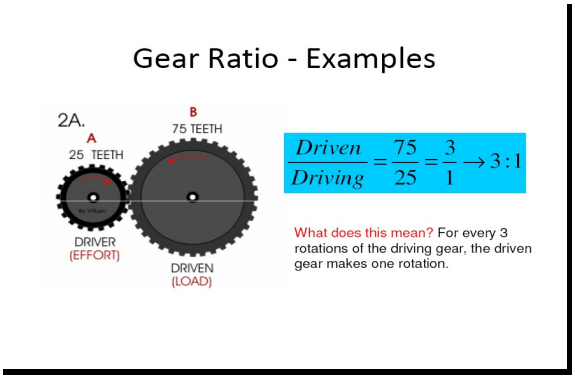

Figure (5.9) shows the gear ratio for controlling the displacement of the collimator in Co-60 in radiotherapy machine

So, specific calculations for gear ratio should be considered to insure that organ motion with collimator displacement is really time.

5.4 Flowchart:

The program start on power ON, resetting all variables, checking data IN from Pressure sensor, refer to the reference value (S). as shown in Figure(5.10) :

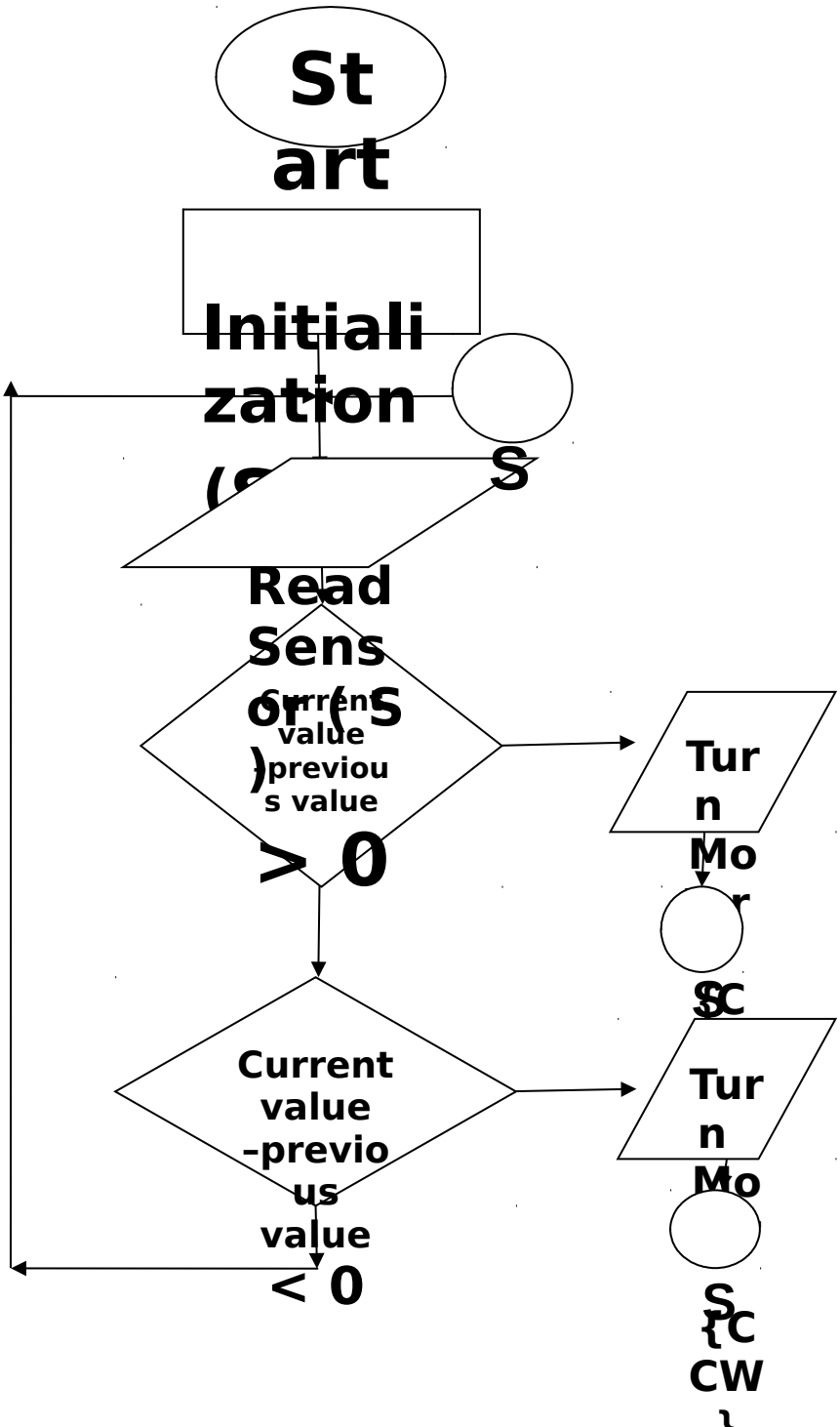

Figure(5.10) shows system flowchart

Chapter Six

System Design And Simulation Results

6.1 The designed system block diagram:

The delay time in any system is directly proportional with numbers of components used, so, least number of components, results in less delay time in the system , this factor be considered in our system design to be really time as follows.

The pressure sensor that selected is the integrated silicon pressure sensor (MPX4250A) that contains signal conditioning stage built in side beside the pressure elements. Also the microcontroller (At mega 16) which consist of ADC built in, has been selected to be one of the constructed components used in the system design in addition to driver(ULN 2003A) circuit and stepper motor, see figure(6.1) that shows the block diagram components used to construct the simulation of the adaptive control system system.

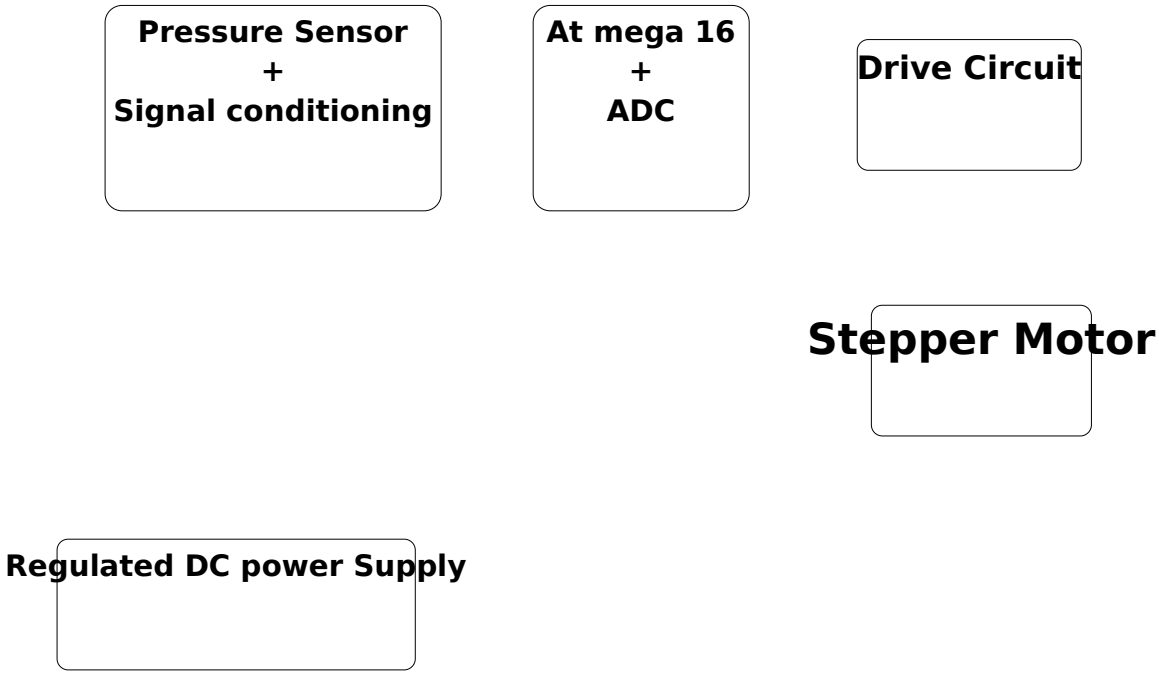

Figure (6.1) Implement circuit block diagram .

6.2 Schematic system diagram :

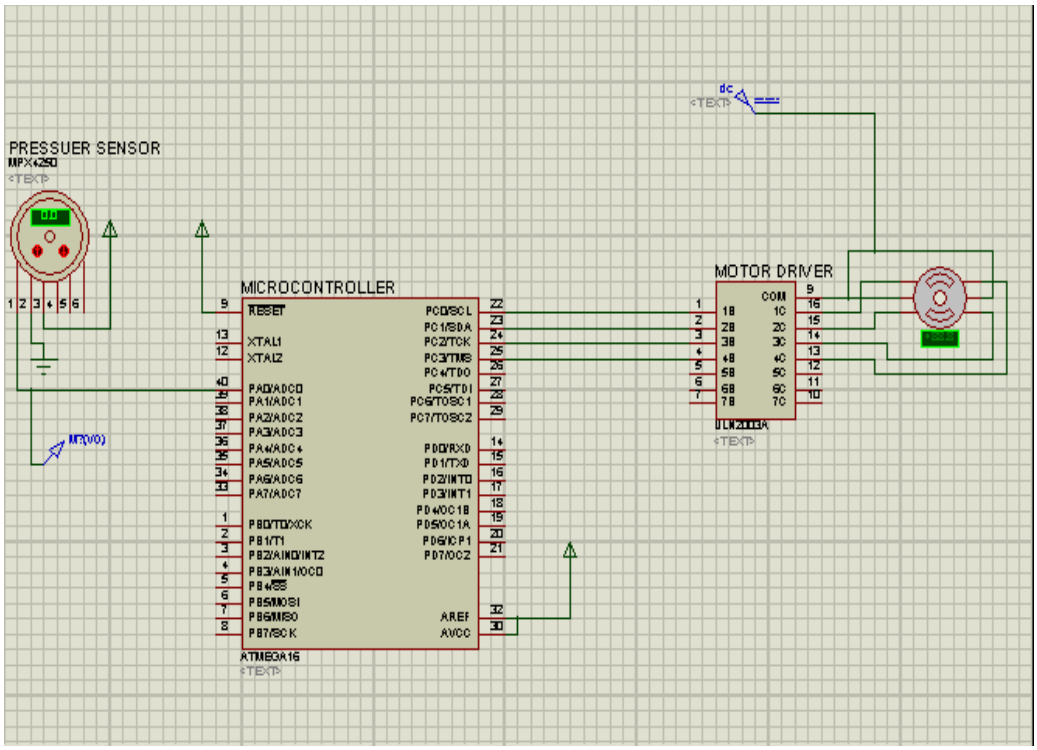

Figure(6.2) Shows the system schematic diagram

See figure (6.3) bellow where X-axes represent the positive pressure values in Kpa when Y-axes represent the grows up voltage generated.

Figure (6.3): Shows the increasing generated voltage during inhalation

On the other hand ,when breathing goes to exhalation state ,this means that the pressure is going to diminish as a result of re-pressing (Negatively) ,as a result the voltage that generated also diminish down from maximum goes to the reference value (zero or S) , in this state (exhalation) , the stepper motor will rotate counter clock wise (CCW) . As in figure (6.4) where X-axes represent the Negative pressure values in Kpa while Y-axes represent the down voltage generated.

Figure(6.4): Shows the decreasing generated voltage during exhalation (negative pressure indicates the abdominal wall retracted down by exhalation pressure.

Figure(6.5) shows and represent the pressuring(inhalation state) and re-pressuring (exhalation state) that generate signal voltage forward and backward (grows up and down) .

Figure(6.5): Shows the state of generated voltage during inhalation and exhalation

5.3 Discussion:

Figure(6.3) shows the generated voltage during inhalation. In which there is increasing generated voltage following the increasing pressure caused by inhalation mechanism, the relationship between the generated voltage and the inhalation pressure could be fitted in the equation of the form: $y = 0.02x + 0.26$, which is so significant as $R^2 = 1$.

Figure (6.4) shows the decreasing generated voltage during exhalation (negative pressure indicates the abdominal wall retracted down by exhalation pressure. The correlation between the generated voltage and the exhalation pressure could be fitted in the equation of the form: $y = - 0.02x + 0.26$, which is significant as $R^2 = 1$. It appears that the generated voltages have equal equation but different direction which indicate and synchronize the mechanism of breathing.

Figure (6.5) shows the state of generated voltage during inhalation and exhalation. The inhalation generates the positive direction volts and the exhalation generates the negative direction volts and the general relationship shoed a polynomial equation of the form: y = 7E-5x2 + 1.09. Such generated voltage could be used to express the mechanism of the breathing and further more to synchronize the abdominal organs motion during radiotherapy, although the breathing pressure will vary from person to another however due to high sensitivity of the integrated silicon pressure sensor, all the signal range could be detected as breathing pressure and converted to voltage.

Figure (6.6) represent two samples of signal voltage output generated due to breathing (Inhalation and Exhalation) which may be different to some extent from some person to an other, depend up on how depth of breathing (Pressure) beside the frequency rate (Acceleration of breathing rate) that represent the duration time (T) .

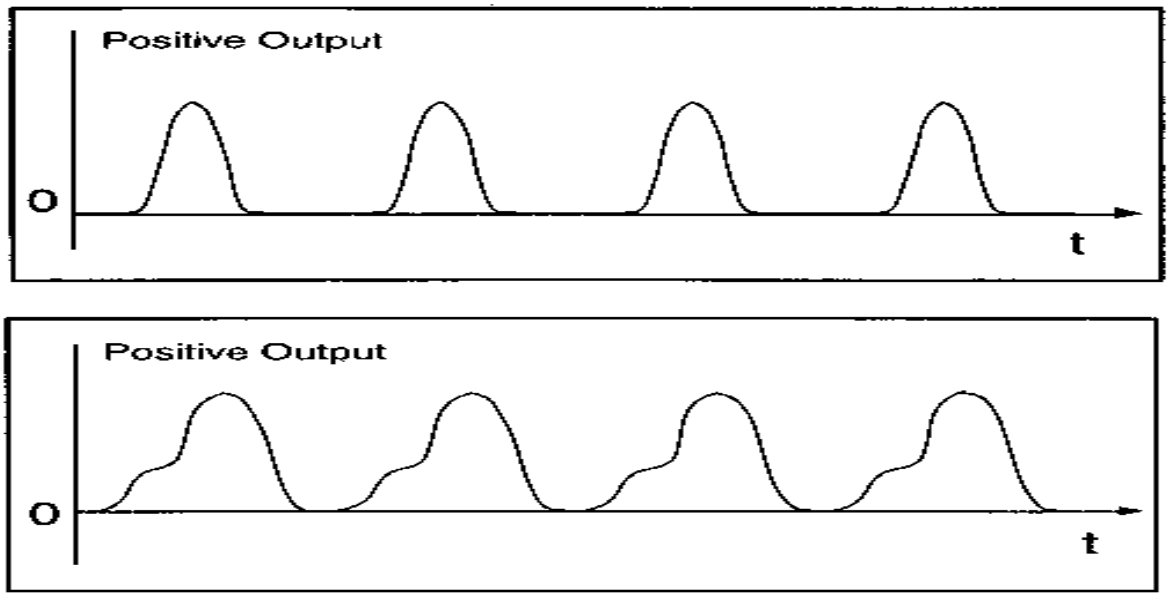

Figure (6.6) Pressure sensor output signal.

As a result, the higher the pressure the higher the signal voltage generated (depend upon breathing pressure) so, more rotation of stepper motor, thus more displacement to the collimator and vise versa.

Figure (6.7) shoes the ideal output signal with amplitude (0 to 5) volt against pressure (0 to 250) kpa pressing and re-pressing spreaded at duration time (T).

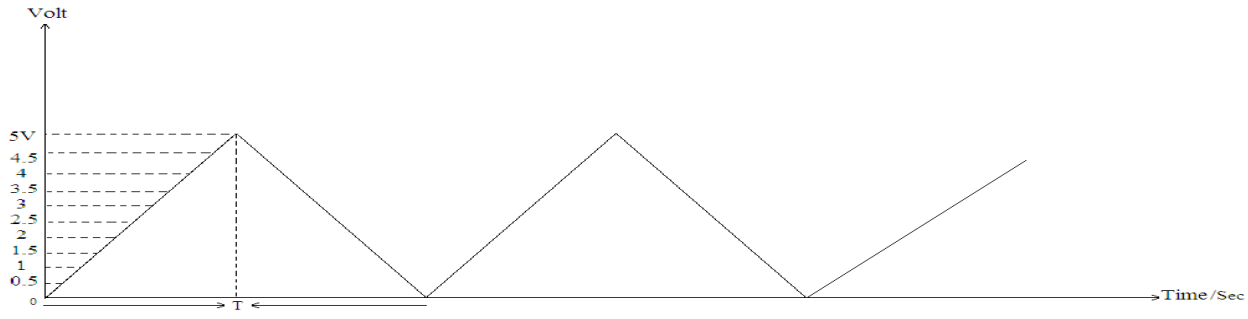

Figure (6.7) Shows the ideal pressure sensor generated signal.

Figure (6.8) illustrate the state of the motor at starting (Stop at 0^0) when reference pressure adjusted to 19 Kpa .

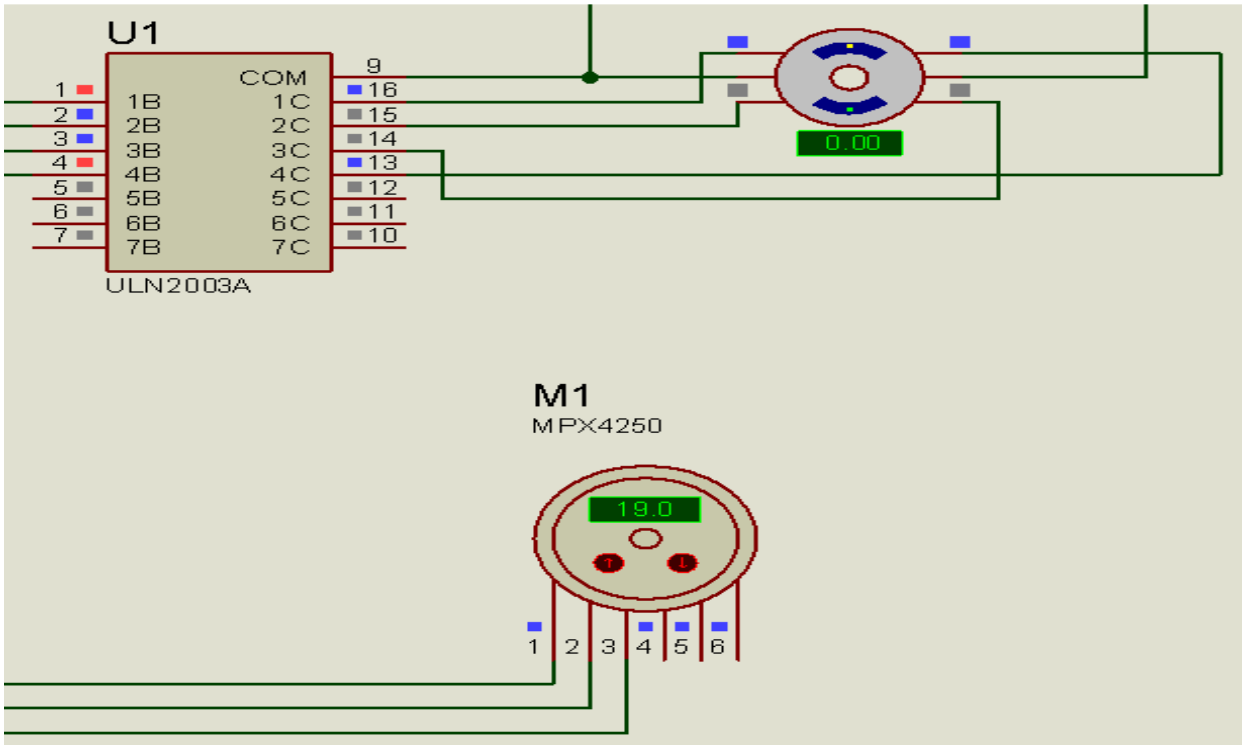

Figure (6.8) Shows the stepper motor At 0^0 when reference pressure was 19 Kpa.

As shown in figure (6.9), when the pressure applied grow up from 19 Kpa to 20 Kpa , the stepper rotate clockwise from 0^0 to + 90^0 .

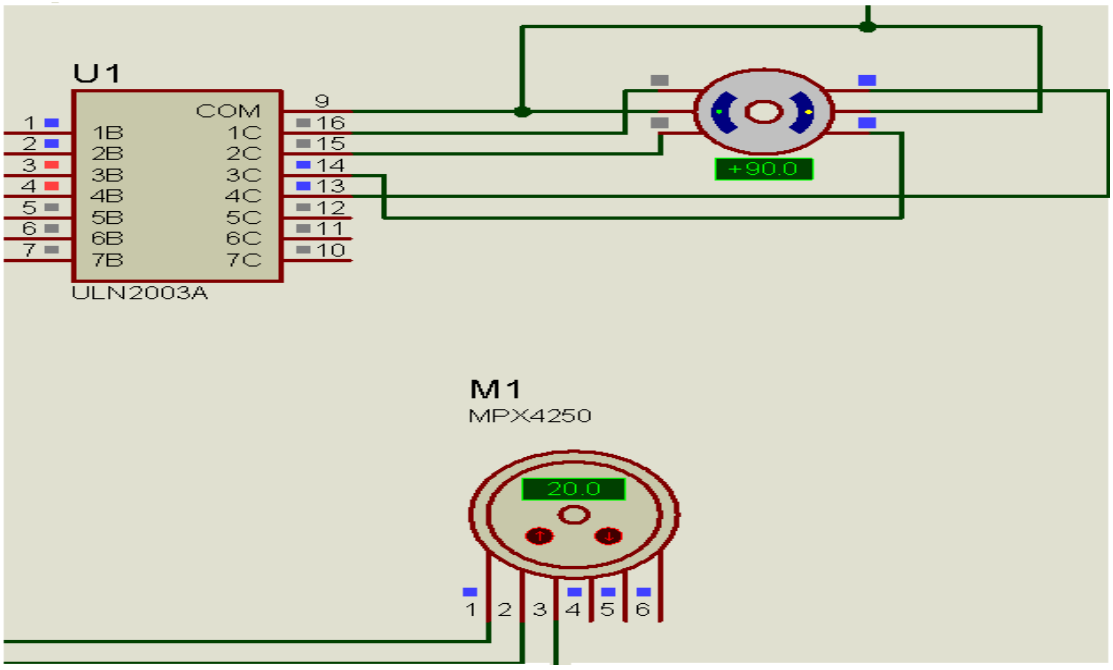

Figure (6.9) Shows the direction rotation of the stepper Motor 90^0 At pressure 20 Kpa

Also when the pressure changed from 20 Kpa to 21 Kpa , the stepper motor rotate clock wise from + 90^0 to + 180^0 as shown in figure (6.10).

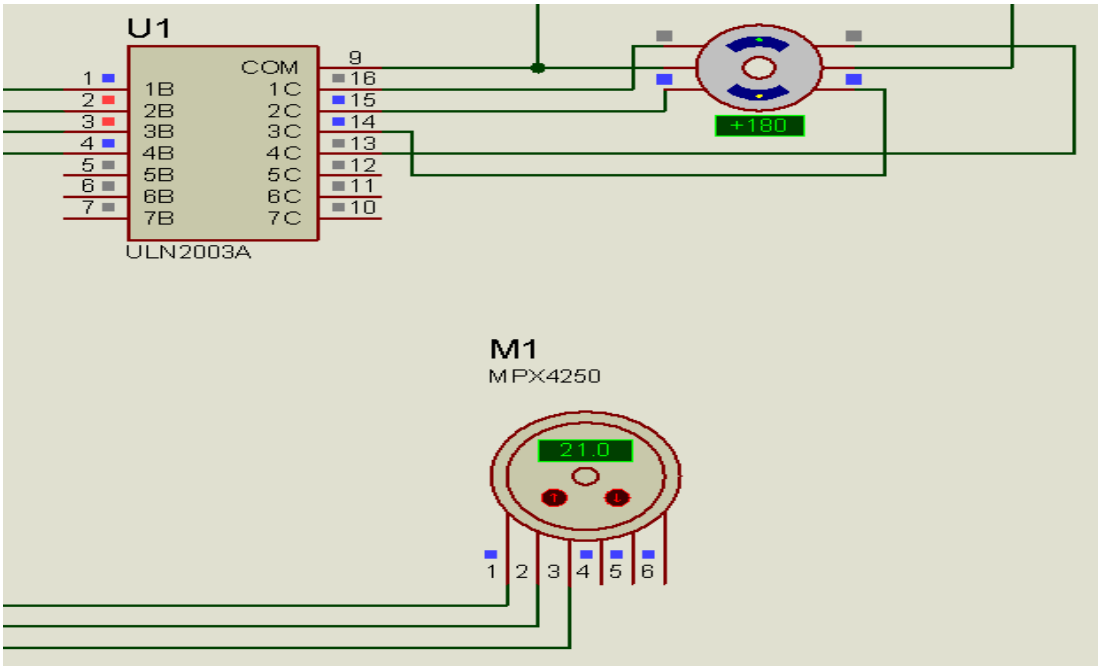

Figure (6.10) Shows the direction rotation of the stepper Motor 180^0 At 21 Kpa.

As seen in figure (6.11) when the pressure applied ,changed positively from 21Kpa to 22Kpa ,the stepper motor rotate in clock wise direction from +180^0 to + 270^0 .

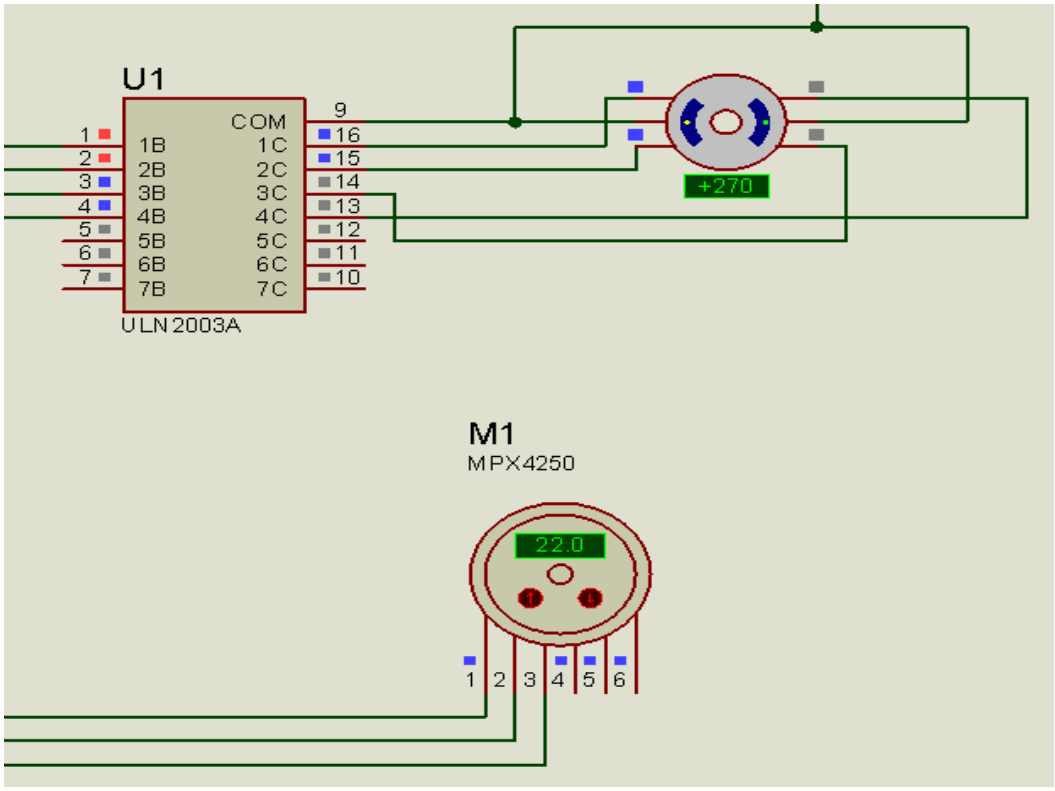

Figure (6.11) Shows the direction of rotation of the stepper Motor 270^0 At 22 Kpa .

The samples seen above determines that the motor rotate clock wise when positively pressed beginning with pressure reference 19 Kpa .

On the other hand, the same thing will occur when re-pressing the pressure sensor, the voltage will retreat back (diminishing) gradually and linearly. As a result the stepper motor will rotate anti clock wise as seen in the simulation application program results.

The process above has been approved according to the conditions written in the conditions mentioned in the paragraph (Methodology) which represent the flaw chart.

According to the simulation results we notice that, pressure of 250 Kpa generates 5v.

Also as a result, the displacement caused due to breathing affect (Inhalation and Exhalation), for Lung and Liver (Tumor movement) in a range of (2 3) Cm maximum.

Also as a fact that should be considered, the frequency rate of the breathing for normal human being, is less than 0.5 Hz.

So the pressure caused by the abdomen and the voltage signal generated against the displacement of the tumor can be represented as shown in the formula below:

250 Kpa 5v 2cm .....(3)

Table (6.1) represents the pressure applied in Killo Pascal and the displacement in Centimeter resulted from that pressure.

Table (6.1) Pressure applied and displacement of collimator.

Pressure (Kpa)	**Displacement (cm)**
0	0
25	0.2
50	0.4
75	0.6
100	0.8
125	1.0
150	1.2
175	1.4
200	1.6
225	1.8

250	2.0

Figure (6.12) represent the relationship between the pressure applied and the displacement (Movement) of the tumor during respiration effect.

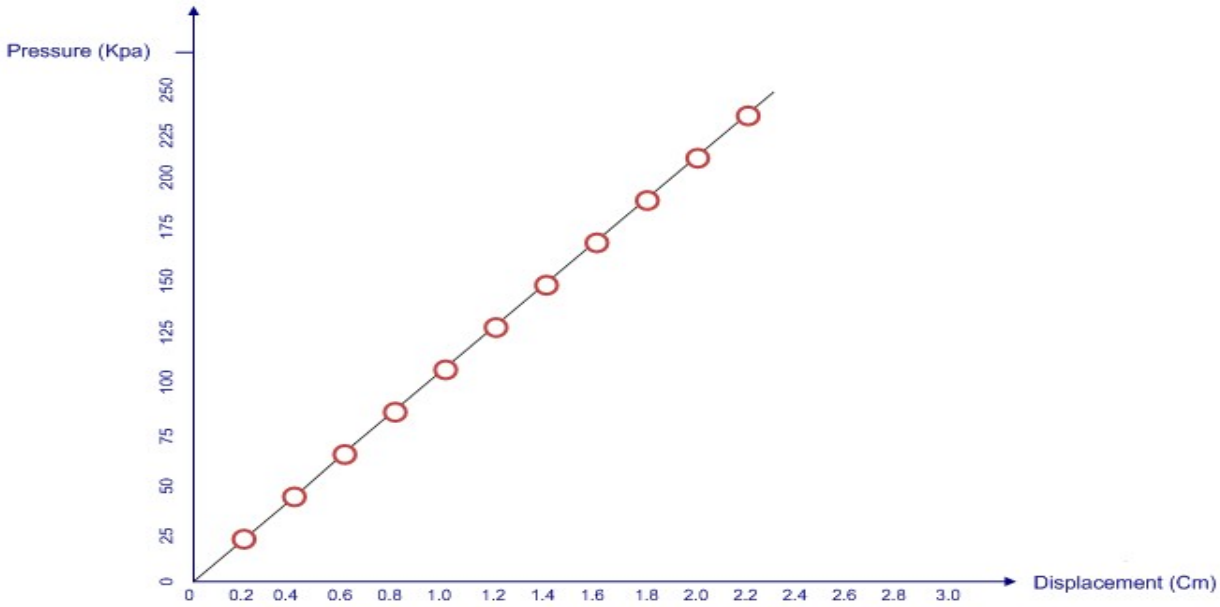

Figure (6.12) pressure applied against displacement.

Also the signal voltage generated can be plotted against the displacement (Movement) of the tumor in figure (6.12) bellow:

5v 2 cm.....(4)

Table (6.2) Consist of grow up voltage and collimator displacement.

Voltage output(V)	**Displacement(Cm)**
0	0
0.5	0.2
1.0	0.4
1.5	0.6
2.0	0.8

2.5	1.0
3.0	1.2
3.5	1.4
4.0	1.6
4.5	1.8
5.0	2.0

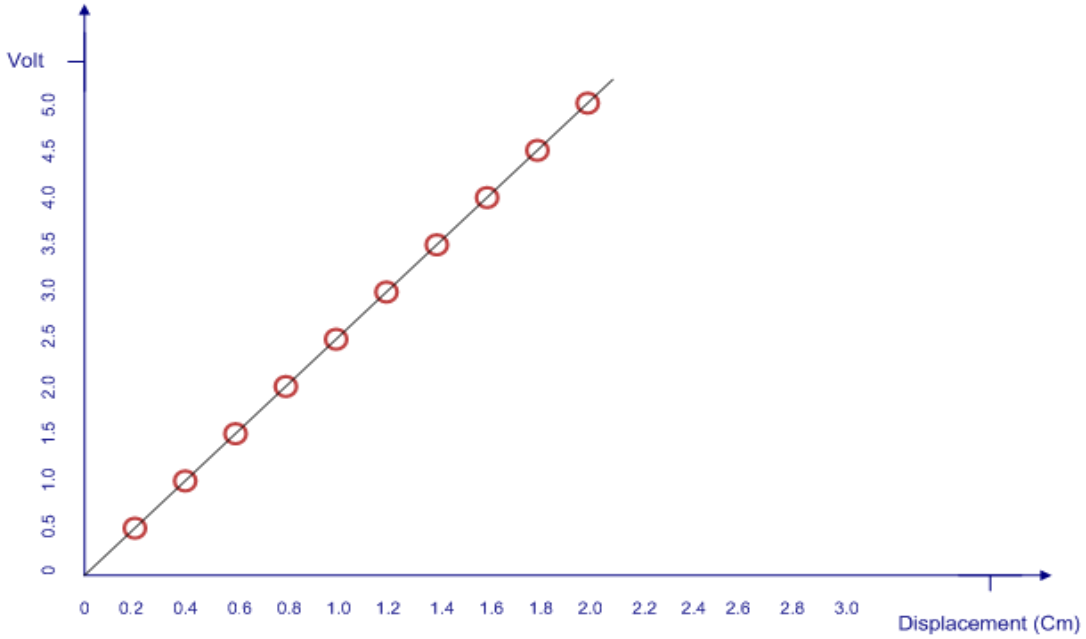

Figure (6.13) Relationship between voltage generated and the displacement.

Gear box attached (Meshed) with the stepper motor to synchronies and translate to control the rotation of the stepper motor to give the required displacement.

The collimator rectangular shape is adjusted manually to specific aria according to the tumor volume when breathing at exhalation state (Minimum aria) , then the stepper motor of the collimator supplied with the electronic circuit designed output voltage using wiring cable ,to make the stepper motor rotate clockwise and counter clockwise , thus the collimator aria move (hesitate) between minimum an maximum aria during breathing in Exhalation and Inhalation state respectively as shown in figure (6.14) .

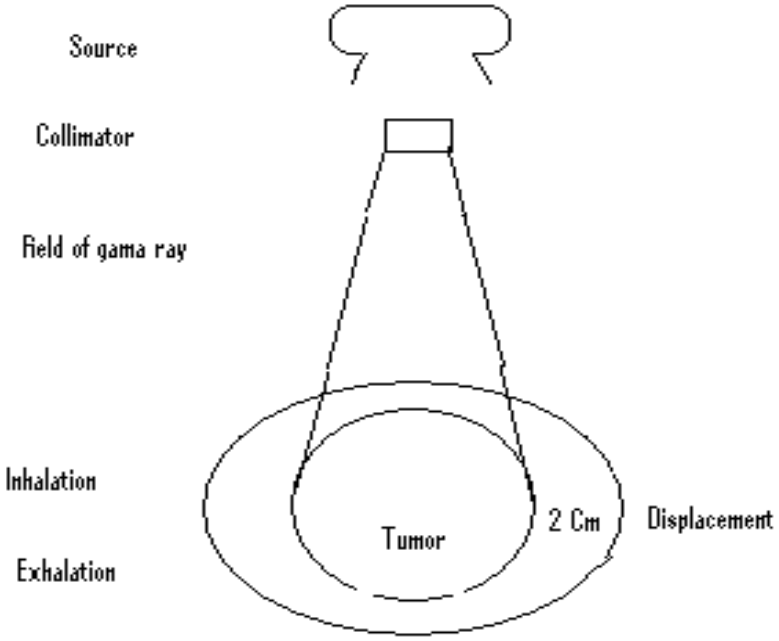

Figure (6.14) The tumor displacement and collimator manual adjustment.

As a result , the rotation of the stepper motor (CW) and (CCW) makes the collimator move in a distance about 2 cm forward and backward , that is to say open to maximum & return again (close) to the reference position (Adjusted point) .Figure (6.14) consist of three diagrams , represent the relation ship between the pressure applied from the abdomen against the pressure sensor and the voltage signal generated and the displacement of the collimator which is done in the same time (Really time) as shown in figure (6.15) :

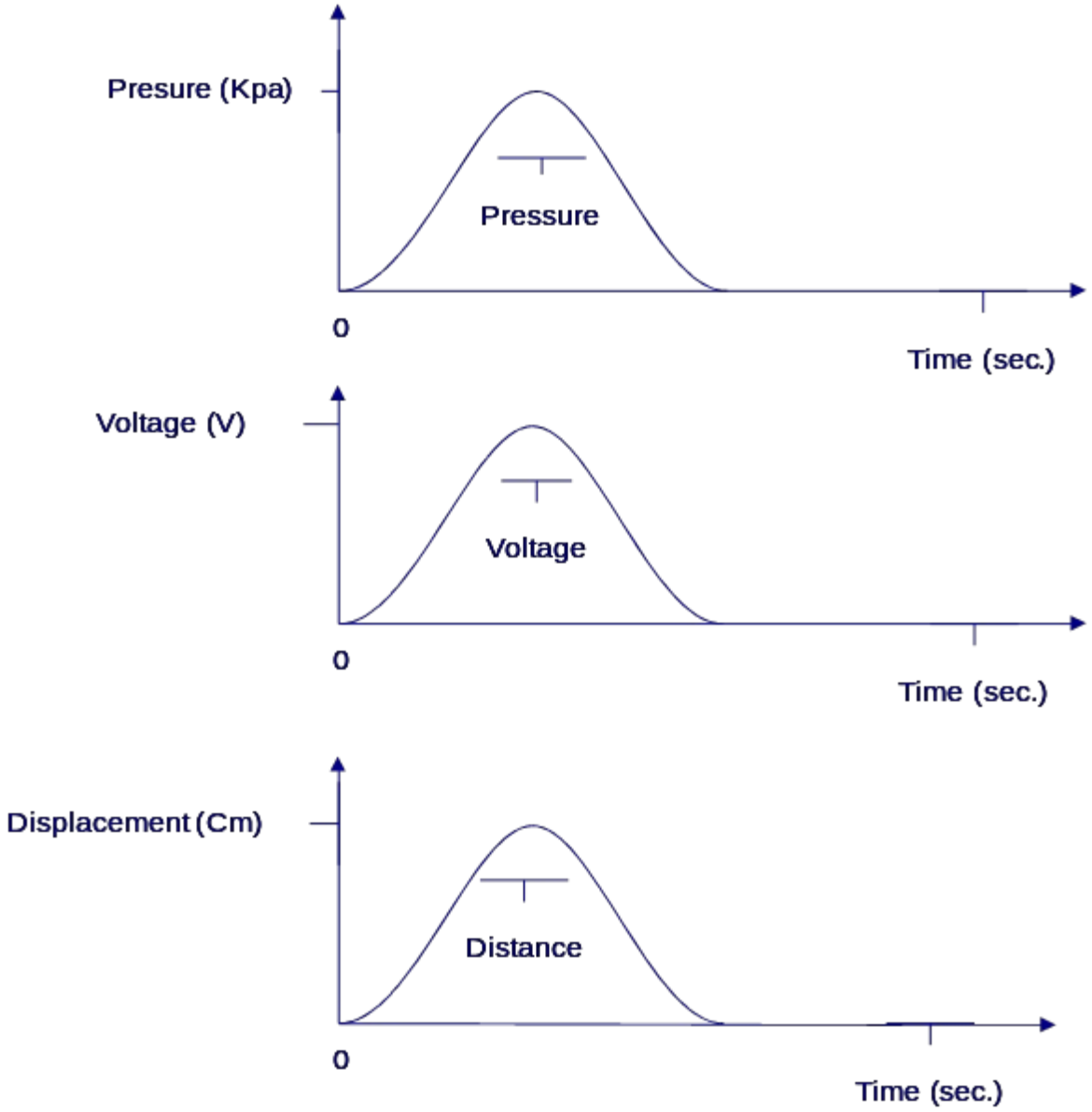

Figure (4.15) Shows the real time between Pressure, Voltage and Displacement.

So that , the movement of the collimator can simulate at really time (Mimic) the movement of the tumor due to the breathing during radiotherapy using Cobalt– 60 machine as simulation reading results determine that .

Some authors (researchers) attempts to solve and overcome the problem of organ motions using deferent mechanical methods , unfortunately there is shortness and drawback to attemption

used as reviewed in Chapter Two , so in this thesis an intelligent electronic method used instead of mechanical ones to make the radiation field just cover specifically the tumor volume (TV) during breathing process really time . This makes the surrounding normal cells (CTV and PTV) are not affected and not been destroyed , while full dose will received by the tumor volume (TV) , this insure that the cancer cells will be fully destroyed , hence reduce the probability of cancer recurrence again .

Chapter Seven

Conclusion And Recommendations

7.1Conclusion:

Radiotherapy treatment is so important in the realm of cancer deices using Copalt-60 machine. Suffering occurred when the tumor under treatment is in the area affected by respiration (Inhalation and Expiration) that lead to organ motion (Displacement).

So, this project is exceeding attemption to solve the problem caused by organ motion, by designing an adaptive control electronic system.

The physiological motion of the abdomen caused by breathing mechanism could be successfully converted into electrical signal and further more could be utilized to synchronize between abdominal organs motion and the radiotherapy field which is stand as one of radiotherapy problem.

An adaptive electronic control system designed and constructed to translate the mechanical movement of the abdomen or a chest into electrical signal (pulses) then supplied to the collimator (Diaphragm) after the later been adjusted manually to the tumor volume (area) to make the collimator move and displace as the movement and displacement of the organ (Tumor) at the same time (Really time) . This circuit designed mainly from pressure sensor, microcontroller, driver circuit ,

gearbox and stepper motor (Highly response time). The simulation results are accepted, that is to say, with enhancement of pressure sensor, the microcontroller, driver circuit and the gear box, the mechanical motion of abdomen due to breathing has been converted into electrical signal in a real time to synchronize the movement of radiotherapy machine diaphragm with target volume motion.

7.2 Recommendations:

The recommendations of this research are to:

1- Construct and implement the designed system in the field of Co-60 radiotherapy machine X-jaws and Y-jaws collimator.
2- Implement an intelligent fuzzy logic system for having more accurate results in multi directions.
3- Chose the best and suitable gearbox coupled with the stepper motor to insure accurate displacement for the collimator diaphragm.
4- Use imaging signal processing to track (tracing) the displacement of tumor volume then translate it to the collimator as electrical pulses at real time .
5- Connect the output pulsating signal resulting from abdominal motion to the multi leaf collimator to make it mimic the tumor volume really time.
6- Minimize the circuit system devices (Components) as possible to reduce time delay if any.

References:

{1} Andre´ De Troyer, Peter A. Kirkwood, and Theodore A. Wilson. (2005). Respiratory Action of the Intercostal Muscles. Physiol Rev 85, P: 717–756.

{2} Balter, J. M., K. L. Lam, C. J. McGinn, T. S. Lawrence, and R. K. Ten Haken, 1998, Improvement of CT-based treatment-planning models of abdominal targets using static exhale imaging, International Journal of Radiation Oncology and Biology Physics,vol.41(4):P.p.939–943.

{3} Bosmans, G., van Baardwijk, A., Dekker, A., Ollers, M., Boersma, L., Minken, A., Lambin, P., Ruysscher, D.D., 2006, Intra-patient variability of tumor volume and tumor motion during conventionally fractionated radiotherapy for locally advanced nonsmall- cell lung cancer: A prospective clinical study, International Journal of Radiation Oncology and Biology Physics, Vol.66,P.p.748-753.

{4} Erridge, S. C., Y. Seppenwoolde, S. H. Muller, M. van Herk, K. De Jaeger, J. S. Belderbos, L. J. Boersma, and J. V. Lebesque, 2003, Portal imaging to assess set-up errors, tumor motion and tumor shrinkage during conformal radiotherapy of non-small cell

lung cancer, Journal of Radiotherapy and Oncology, Vol.66(1):P.p.75–85.

{5} Estenne M. and De Troyer A. (1985). Relationship between respiratory muscle electromyogram and rib cage motion in tetraplegia. Am Rev Respir Dis. Vol. 132, P: 53–59.

{6} Gandevia SC, Leeper JB, McKenzie DK, and De Troyer A. (1996). Discharge frequencies of parasternal intercostal and scalene motor units during breathing in normal and COPD subjects. Am J Resp Crit Care Med, Vol. 153, P: 622–628.

{7} Harauz, G., and M. J. Bronskill, 1999, Comparison of the liver's respiratory motion in the supine and upright positions: Concise communication, Journal of Nuclear Medicine, Vol.20(7):P.p.733–573.

{8} International Commission on Radiation Units and Measurements. (1993). Prescribing, recording and reporting photon beam therapy. ICRU Report 50.

{9} International Commission on Radiation Units and Measurements. (1999). Prescribing, recording and reporting photon beam therapy. (Supplement to ICRU report 50). ICRU Report 62.

{10} Joshi C P, Darko J, Vidyasagar P B and Schreiner L J. Investigation of an efficient source design for Cobalt-60-based tomotherapy using EGSnrc Monte Carlo simulations Phys. Med. Biol. 53, 575, (2008).

{11} Jun Xu, Nikos Papanikolaou, Chengyu Shi and Steve B Jiang. Synchronized moving aperture radiation therapy (SMART): superimposing tumor motion on IMRT MLC leaf sequences under realistic delivery conditions. Phys. Med. Biol. 54 4993, (2009).

[12} Keall, P. J., G. Starkschall, H. Shukla, K. M. Forster, V. Ortiz, C. W. Stevens, S. S. Vedam, R. George, T. Guerrero, and R. Mohan,2004, Acquiring 4D thoracic CT scans using a multislice helical method,Journal of Medical Physics and Biology, vol.49(10):P.p.2053–2067.

{13} Kitamura, K., H. Shirato, Y. Seppenwoolde, R. Onimaru, M. Oda, K. Fujita, S. Shimizu, N. Shinohara, T. Harabayashi, and K. Miyasaka. (2002) “Three-dimensional intrafractional movement of prostate measured during real-time tumor-tracking radiotherapy in supine and prone treatment positions.” Int J Radiat Oncol Biol Phys 53(5):1117–1123.

{14} Li, T., Schreibmann, E., Thorndyke, B., Tillman, G., Boyer, A., Koong, A., Goodman, K., Xing, L.: (2005). Radiation dose reduction in four-dimensional computed tomography, Journal of Medical Physics and Biology,vol.32, P.p.3650-3660.

{15} Mageras, G. S., and E. Yorke, 2004, Deep inspiration breath hold and respiratory gating strategies for reducing organ motion in radiation treatment, Semin Radiation Oncology Journal, Vol.14(1):P.p.65–75.

{16} Malone, S., J. M. Crook, W. S. Kendal, and J. Szanto. “Respiratory-induced prostate motion: quantification and characterization.” Int J Radiat Oncol Biol Phys 48(1):105–109, (2000).

{17} McCarter SD, Beckhan WA. (2000). Evaluation of the validity of a convolution method for incorporating tumour movement and set-up variation into the radiotherapy treatment planning system. Phys Med Biol. ; Vol. 45, P: 923–931.

{18} Prince, J.L., Links, J.M., 2006, Medical imaging signals and systems. Prentice-Hall Ltd, England.

{19} Rit, S., Wolthaus, J., van Herk, M., Sonke, J.J.: On-the-y motion-compensated cone-beam CT using an a priori motion model. In: Medical Image Computing and Computer Assisted Intervention (MICCAI), Journal of Medical Physics and Biology,vol.5241, P.p.729-736.

{20} Sergio Diez, Javier Garcia, Francisco Sendra. (2004). Analysis and evaluation of periodic physiological organ motion in radiotherapy treatments. Radiotherapy and Oncology Vol. 73, P: 325–329.

{21} Seungwoo Park, Haijo Jung, Kum Bae Kim, Donghan Lee and Young Hoon J. (2009). Development and Evaluation of a Target-tracking Radiation-therapy System Using a Multileaf Collimator (MLC) Synchronized with Moving Organs. Journal of the Korean Physical Society, Vol. 55, No. 2, pp. 694 – 701.

{22} Sitharama S. Lyengar, Nandan P. , Vir V., Phoha, N. Balakrishnan. (2010). Fundamental of Sensor Network Programming: Application and Technology, Wiley-IE.EE Press.

{23} Sonke, J., L. Zijp, P. Remeijer, and M. van Herk, 2005, Respiratory correlated cone beam CT,Journal of Medical Physics and Biology, vol.32(4):P.p.1176–1186.

{24} Stam, J, 2001, A simple quid solver based on the FFT. Journal of Graphics Tools Vol.6,P.p.383-396.

{25} Strohl KP, Mead J, Banzett RB, Lehr J, Loring SH, and O'Cain CF. (1984). Effect of posture on upper and lower rib cage motion and tidal volume during diaphragm pacing. Am Rev Respir Dis, Vol. 130, P: 320–321.

{26} Su Y, M H Fisher and R S Rowland. (2007). Marker-less Intra-Fraction Organ Motion Tracking – A Hybrid ASM Approach. IEEE International Workshop on Imaging Systems and Techniques, May 4–5, Krakow, Poland.

{27} Underberg, R. W., F. J. Lagerwaard, B. J. Slotman, J. P. Cuijpers, and S. Senan, 2005, Use of maximum intensity projections (MIP) for target volume generation in 4DCT scans for lung cancer, International Journal of Radiation Oncology and Biology Physics,vol.63(1):P.p.253–260.

{28} Urie MM, Goitein M, Doppke K, (1991). The role of uncertainty analysis in treatment planning. In t J Radiat Oncol Biol Phys. Vol. 21, P: 91–107.

{29} Weiss, E., H. Vorwerk, S. Richter, and C. F. Hess. (2003). "Interfractional and intrafractional accuracy during radiotherapy of gynecologic carcinomas: A

comprehensive evaluation using the ExacTrac system.” Int J Radiat Oncol Biol Phys 56(1):69–79.

{30} West, J. B. Respiratory Physiology: (1974). The Essentials. Baltimore, MD: Waverly Press, Inc.

{31} Yamamoto, T., Langner, U., Billy W. Loo, J., Shen, J., Keall, P.J.: Retrospective analysis of artifacts in four-dimensional CT images of 50 abdominal and thoracic radiotherapy patients.International Journal of Radiation Oncology and Biology Physics, Vol.72, P.p.1250-1258.

{32} Yu, H., Wang, G., 2007, Data consistency based rigid motion artifact reduction in fanbeam CT. IEEE Trans., Journal of Medical Physics and Biology,vol.26, P.p.249-260.

{33} Holler, F. James; Skoog, Douglas A; Crouch, Stanley R (2007). "Chapter 1". Principles of Instrumental Analysis (6th ed.). Cengage Learning. p. 9. ISBN 978-0-495-01201-6.

{34} a b Manbachi, A. and Cobbold R.S.C. (2011). "Development and Application of Piezoelectric Materials for Ultrasound Generation and Detection". Ultrasound 19 (4): 187–196. doi:10.1258/ult.2011.011027.

{35} Gautschi, G (2002). Piezoelectric Sensorics: Force, Strain, Pressure, Acceleration and Acoustic Emission Sensors, Materials and Amplifiers. Springer.

{36} J. Krautkrämer, and H. Krautkrämer (1990). Ultrasonic Testing of Materials. Springer.

{37} Woldemar Voigt, Lehrbuch der Kristallphysik (Berlin, Germany: B. G. Teubner, 1910).

{38} a b c M. Birkholz (1995). "Crystal-field induced dipoles in heteropolar crystals – II. physical significance". Z. Phys. B 96 (3): 333–340. Bibcode:1995ZPhyB..96..333B. doi:10.1007/BF01313055.

{39} S. Trolier-McKinstry (2008). "Chapter3: Crystal Chemistry of Piezoelectric Materials". In A. Safari, E.K. Akdo˘gan. Piezoelectric and Acoustic Materials for Transducer Applications. New York: Springer. ISBN 978-0-387-76538-9.

{40} Sensor Sense: Piezoelectric Force Sensors. Machinedesign.com (2008-02-07). Retrieved on 2012-05-04.

{41} Damjanovic, Dragan (1998). "Ferroelectric, dielectric and piezoelectric properties of ferroelectric thin films and ceramics". Reports on Progress in Physics 61 (9): 1267–1324. Bibcode:1998RPPh...61.1267D. doi:10.1088/0034-4885/61/9/002.

{42} Kochervinskii, V (2003). "Piezoelectricity in Crystallizing Ferroelectric Polymers". Crystallography Reports 48 (4): 649–675. Bibcode:2003CryRp..48..649K. doi:10.1134/1.1595194

.{43} Akizuki, Mizuhiko, Martin S. Hampar, and Jack Zussman (1979). "An explanation of anomalous optical properties of topaz". Mineralogical Magazine 43 (326): 237–241. doi:10.1180/minmag.1979.043.326.05.

{44} M. Minary-Jolandan, and Min-Feng Yu (2009). "Nanoscale characterization of isolated individual type I collagen fibrils: Polarization and piezoelectricity". Nanotechnology 20 (8): 085706. Bibcode:2009Nanot..20h5706M. doi:10.1088/0957-4484/20/8/085706. PMID 19417467.

{45} Becker, Robert O; Marino, Andrew A (1982). "Chapter 4: Electrical Properties of Biological Tissue (Piezoelectricity)". Electromagnetism and Life. Albany, New York: State University of New York Press. ISBN 0-87395-560-9.

{46} Pollack, S.R, Korostoff, E., Starkebaum, W. y Lannicone, W (1979). "Micro-electrical studies of stress-generated potentials in bone". In Brighton, C.T., Black, J. and Pollack, S.R. Electrical Properties of Bone and Cartilage. New York City: Grune and Stratton, Inc. ISBN 0-8089-1228-3.

{47} Fotiadis, D.I; Foutsitzi, G., and Massalas, C.V (1999). "Wave propagation modeling in human long bones". Acta Mechanica 137: 65–81. doi:10.1007/BF01313145.

{48} Lee, BY; Zhang, J; Zueger, C; Chung, WJ; Yoo, SY; Wang, E; Meyer, J; Ramesh, R; Lee, SW (2012-05-13). "Virus-based piezoelectric energy generation.". Nature nanotechnology 7 (6): 351–6. Bibcode:2012NatNa...7..351L. doi:10.1038/nnano.2012.69. PMID 22581406.

{49} Saito, Yasuyoshi; Takao, Hisaaki; Tanil, Toshihiko; Nonoyama, Tatsuhiko; Takatoril Kazumasa; Homma, Takahiko; Nagaya, Toshiatsu; Nakamura, Masaya (2004-11-04). "Lead-free piezoceramics". Nature (Nature Publishing Group) 432 (7013): 81–87. Bibcode:2004Natur.432...84S. doi:10.1038/nature03028. PMID 15516921.

{50} "Market Report: World Piezoelectric Device Market". Acmite Market Intelligence.

{51} Richard, Michael Graham (2006-08-04). "Japan: Producing Electricity from Train Station Ticket Gates". TreeHugger. Discovery Communications, LLC.

{52} Wright, Sarah H (2007-07-25). "MIT duo sees people-powered "Crowd Farm"". MIT news. Massachusetts Institute of Technology.

{53} Kannampilly, Ammu (2008-07-11). "How to Save the World One Dance at a Time". ABC. ABC.

{54} Phillips, James R (2000-08-10). "Piezoelectric Technology: A Primer". eeProductCenter. TechInsights.

{55} Speck, Shane. (2004-03-11) How Rocket-Propelled Grenades Work by Shane Speck. Science.howstuffworks.com. Retrieved on 2012-05-04.

{56} Le Letty, R.; Barillot, F.; Lhermet, N.; Claeyssen, F.; Yorck, M.; Gavira Izquierdo, J.; Arends, H.; Barillot; Lhermet; Claeyssen; Yorck; Gavira Izquierdo; Arends (2001). "The scanning mechanism for ROSETTA/MIDAS from an engineering model to the flight model". Proceedings of the 9th European Space Mechanisms and Tribology Symposium, 19–21 September 2001, Liège, Belgium. Compiled by R. A. Harris. ESA SP-480, Noordwijk, Netherlands: ESA Publications Division 480: 75–81. Bibcode:2001ESASP.480...75L. ISBN 92-9092-761-5.

{57} Simonsen, Torben R. Piezo in space Electronics Business (in Danish), 27 September 2010. Retrieved: 28 September 2010.

{58} HEAD. Retrieved 2008 "Isn't it amazing how one smart idea, one chip and an intelligent material has changed the world of tennis?".

{59} Baltaci, Volkan; Ayvaz, Özge Üner; Ünsal, Evrim; Aktaş, Yasemin; Baltacı, Aysun; Turhan, Feriba; Özcan, Sarp; Sönmezer, Murat (2009). "The effectiveness of intracytoplasmic sperm injection combined with piezoelectric stimulation in infertile couples with total fertilization failure". Fertil. Steril. 94 (3): 900–4. doi:10.1016/j.fertnstert.2009.03.107. PMID 19464000.

{60} Hoigne DJ, Stubinger S, Von Kaenel O, Shamdasani S, Hasenboehler P. (2006). "Piezoelectic osteotomy in hand surgery: first experiences with a new technique". BMC Musculoskelet Disord 7: 36. doi:10.1186/1471-2474-7-36.

{61} Labanca M, Azzola F, Vinci R, Rodella LF. (2008). "Piezoelectric surgery: twenty years of use". Br J Oral Maxillofac Surg 46 (4): 265–9. doi:10.1016/j.bjoms.2007.12.007. PMID 18342999.

{62} Gautschi, G. (2002). Piezoelectric sensorics. Springer Berlin, Heidelberg, New York.

{63} wali, r paul (OCT 2012). "An electronic nose to differentiate aromatic flowers using a real-time information-rich piezoelectric resonance measurement". Procedia Chemistry: 194–202. doi:10.1016/j.proche.2012.10.146.

{64} March 2006. Retrieved 2007 a b "Interfacing Piezo Film to Electronics" (PDF). Measurement Specialties.

{65} a b c Alfredo Vázquez Carazo (January 2000). Novel Piezoelectric Transducers for High Voltage Measurements. Universitat Politècnica de Catalunya. p. 242.

{66} Karki, James (September 2000). "Signal Conditioning Piezoelectric Sensors" (PDF). Texas Instruments. Retrieved 2007-12-02.

{67} Ludlow, Chris (May 2008). "Energy Harvesting with Piezoelectric Sensors" (PDF). Mide Technology. Retrieved 2008-05-21.[dead link]

{68} Knoll, Glenn F. (1989). Radiation Detection and Measurement (2nd ed.). New York: John Wiley & Sons. ISBN 0471815047.

{69} Nicholson, P. W. (1974). Nuclear Electronics. New York: John Wiley & Sons. pp. 315–316. ISBN 0471636975.

{70}ttp://www.engineersgarage.com/electronic-components/atmega16-microcontr. 2012 EngineersGarage.

{71} Wikipedia. Servo | wikipedia, die freie enzyklop□adie, 2011. [Online; Stand 23. November 2011.

{72}San José. State University Dept. of Mechanical and Aerospace Engineering rev. 3.4 06 SEP 2010.

{73} https://www.google.com/ Ligo George. electrosome.com/uln2003-high-voltage-current-driver/ - Feb 24, 2013.

.